Neurobiology of Stress 15 (2021) 100373

Contents lists available at ScienceDirect

Neurobiology of Stress

journal homepage: www.elsevier.com/locate/ynstr

LGI1 governs neuritin-mediated resilience to chronic stress

Seung Hoon Lee [a,b,1], Nam-Shik Kim [c,d,1], Miyeon Choi [e], Seung Yeon Ko [e], Sung Eun Wang [f], Hye-Ryeong Jo [e], Jee Young Seo [a], Yong-Seok Kim [a,b], Hyun Jin Kim [c], Hyun-Yong Lee [c], Joung-Hun Kim [c,**], Hyeon Son [a,b,*]

[a] Graduate School of Biomedical Science and Engineering, Hanyang Biomedical Research Institute, Hanyang University, 222 Wangsimni-ro, Seongdong-gu, Seoul, Republic of Korea
[b] Department of Biochemistry and Molecular Biology, College of Medicine, Hanyang University, 222 Wangsimni-ro, Seongdong-gu, Seoul, Republic of Korea
[c] Department of Life Sciences, Pohang University of Science and Technology (POSTECH), 77 Cheongam-Ro, Namgu, 37673, Pohang, Republic of Korea
[d] Department of Biological Sciences, Korea Advanced Institute of Science and Technology (KAIST), 34141, Daejeon, Republic of Korea
[e] Hanyang Biomedical Research Institute, Hanyang University, Seongdong-gu, Seoul, Republic of Korea
[f] Department of Genetics, Yale University School of Medicine, 333 Cedar Street, New Haven, CT, 06520, USA

ARTICLE INFO

Keywords:
LGI1
Neuritin
Depression
HDAC5
MEF2D
Hippocampus

ABSTRACT

Depression is accompanied by neuronal atrophy and decreased neuroplasticity. Leucine-rich glioma-inactivated protein 1 (LGI1), a metastasis suppressor, plays an important role in the development of CNS synapses. We found that LGI1 expression was reduced in the hippocampi of mice that underwent chronic unpredictable stress (CUS), and could be rescued by the antidepressant, fluoxetine. Recombinant soluble neuritin, an endogenous protein previously implicated in antidepressant-like behaviors, elevated hippocampal LGI1 expression in a manner dependent on histone deacetylase 5 (HDAC5) phosphorylation. Accordingly, *Nrn1* $^{flox/flox}$*;Pomc-cre* (*Nrn1* cOE) mice, which conditionally overexpress neuritin, displayed increases in hippocampal LGI1 level under CUS and exhibited resilience to CUS that were blocked by hippocampal depletion of LGI1. Interestingly, neuritin-mediated LGI1 expression was inhibited by HNMPA-$(AM)_3$, an insulin receptor inhibitor, as was neuritin-mediated HDAC5 phosphorylation. We thus establish hippocampal LGI1 as an effector of neurite outgrowth and stress resilience, and suggest that HDAC5-LGI1 plays a critical role in ameliorating pathological depression.

1. Introduction

Stress is linked to depression and has been connected with multiple neuronal changes in key brain regions involved in depression. Exposure to chronic stress is often used to elicit depressive-like behaviors in animal models (Stepanichev et al., 2014). Mice subjected to chronic unpredictable stress (CUS) exhibit neuronal and behavioral deficits such as cellular and synaptic atrophy of neuronal populations in various brain regions including the hippocampi (Nestler and Hyman, 2010). However, the molecular and cellular mechanisms underlying the elimination of synapses and neurites remain unclear.

Leucine-rich glioma-inactivated protein 1 (LGI1) is a secreted protein that is a Nogo receptor 1 (NgR1) ligand. LGI1 is expressed in neurons throughout the brain, but is enriched in the hippocampus (Kegel et al., 2013). At the cellular level, it is present in presynaptic boutons (Boillot et al., 2016), and NgR1 and its coreceptor, tumor necrosis factor receptor orphan Y (TROY), are also expressed in the dendrites of hippocampal neurons (Thomas et al., 2018). Incubation of cultured neurons with LGI1 increases the formation of synapses and mushroom-type spines (Thomas et al., 2018). LGI1 also regulates post synaptic density 95 protein (PSD95) and glutamate receptor (GluR) channels, and enhances neurite outgrowth in vitro and *in vivo* (Lovero et al., 2015; Owuor et al., 2009).

Neuritin (*Nrn1*), otherwise known as candidate plasticity gene 15 (CPG15), promotes neurite outgrowth (Fujino et al., 2008; Lee et al., 2005; Naeve et al., 1997), neuronal migration (Zito et al., 2014), spine

* Corresponding author. College of Medicine, Hanyang University, 222 Wangsimni-ro, Seongdong-gu, Seoul, 04763, Republic of Korea
** Corresponding author.
E-mail addresses: lsh2012@hanyang.ac.kr (S.H. Lee), namshikkim1@gmail.com (N.-S. Kim), liebemy@hanyang.ac.kr (M. Choi), seungyeon430@gmail.com (S.Y. Ko), sungeun.wang@yale.edu (S.E. Wang), jhr1086@gmail.com (H.-R. Jo), jyseo1205@hanyang.ac.kr (J.Y. Seo), yongsk@hanyang.ac.kr (Y.-S. Kim), hanzlight@postech.ac.kr (H.J. Kim), elliotlee@postech.ac.kr (H.-Y. Lee), joungkim@postech.ac.kr (J.-H. Kim), hyeonson@hanyang.ac.kr (H. Son).
[1] S.H.L. and N.-S.K. contributed equally to this work.

https://doi.org/10.1016/j.ynstr.2021.100373
Received 20 April 2021; Received in revised form 26 July 2021; Accepted 27 July 2021
Available online 28 July 2021

maturation (An et al., 2014; Choi et al., 2014; Son et al., 2012) and axonal regeneration (Karamoysoyli et al., 2008). Importantly, it rescues stress-induced depressive-like behaviors, and prevents the atrophy of dendrites and dendritic spines caused by chronic stress (Son et al., 2012). Given our previous observations, we hypothesized that LGI1 mediates neuritin-induced neuritogenesis through its activity-dependent effects in neurons and enrichment in the hippocampus, a key brain region implicated in stress responses (McEwen et al., 2015).

To test this idea, we examined the role of LGI1 in a mouse model of depression. We found that neuritin-induced neurite outgrowth was indeed dependent on LGI1. Moreover, *Nrn1* cOE mice, which conditionally overexpress neuritin, exhibited antidepressant-like behaviors when neuritin was expressed that were abolished by blockade of LGI1 expression.

2. Materials and methods

2.1. Generation of mice conditionally overexpressing Rosa26-Flag-neuritin

A targeting vector was designed to knock in a cassette that permits conditional expression of Flag-tagged *Nrn1* cDNA into the *Rosa26* locus of the mouse genome, and constructed as described (Srinivas et al., 2001). Once the floxed tPA (transcriptional stop) has been removed by Cre recombinase, the Rosa promoter drives *Nrn1* cDNA transcription. The targeting vector was electroporated into mouse embryonic stem cells, and targeted clones were selected by PCR and injected into C57BL/6J blastocysts. Confirmation of germ-line transmission of the floxed allele and future genotyping were performed by PCR from tail genomic DNA with two genotyping primers. The mice were backcrossed to C57BL/6J at least 5 times before all the experiments.

2.2. Mice

All experiments were conducted with 8–12 week male C57BL/6 mice (Koatech, Pyeongtaek, Korea), $Nrn1^{flox/flox}$ (control) male mice and $Nrn1^{flox/flox}$; *Pomc-cre* (*Nrn1* cOE) male mice. FVB-*Pomc-cre* mice [B6. FVB-Tg (*Pomc-cre*)1Stl/J (#010714)] were obtained from the Jackson Laboratory (Bar Harbor, ME, USA). They were backcrossed to C57BL/6 mice for more than 12 generations (https://www.jax.org/strain/010714). $Nrn1^{flox/flox}$ female mice were crossed with FVB-*Pomc-cre* male mice to generate neuritin overexpressing male mice ($Nrn1^{flox/flox}$; *Pomc-cre*, *Nrn1* cOE), and genotypes were confirmed by PCR analysis. All animals were maintained in a humidity-controlled environment (12 h light/dark cycle) with access to food and water ad libitum. All animal experiments were approved by the Institutional Animal Care and Use Committee of the Hanyang University (Seoul, Korea) and were performed in accordance with relevant guidelines and regulations.

2.3. Culture of primary hippocampal neurons

Hippocampi from E14.5 C57BL/6 mice embryos were rapidly and aseptically dissected into ice-cold Ca^{2+}/Mg^{2+}-free Hanks balanced salt solution (HBSS; Gibco, Carlsbad, CA, USA), followed by removal of meninges and mincing into small pieces. The hippocampal tissue was then digested with 0.05% Trypsin-EDTA (Welgene, Daegu, Korea) for 5 min at 37 °C, and digestion was stopped with neurobasal (NB) medium (Gibco) with 10% fetal bovine serum (FBS, Gibco), 0.5 mM L-glutamine (Sigma Aldrich, St Louis, MO, USA) and 100X penicillin/streptomycin (Welgene). After centrifugation at 200×*g* for 1 min, the pelleted cells were gently resuspended in NB medium with 10% fetal bovine serum, and plated at 50,000–60,000 cells per cm^2 on culture dishes coated with 25 μg/ml poly-L-lysine (Sigma Aldrich) in PBS and 10 μg/ml laminin (Invitrogen, Carlsbad, CA, USA) in PBS. Hippocampal primary neuronal cells were grown for 1 day in NB medium with 10% FBS, 0.5 mM L-glutamine, and 1% 100X penicillin-streptomycin. Next day, the medium was replaced with NB medium containing 2% B27 serum-free supplement (Gibco), 0.5 mM L-glutamine, and 1% 100X penicillin/streptomycin. Cultures were maintained for 7–12 d at 37 °C in an incubator with 5% CO_2.

2.4. Drug treatment

On days-in-vitro (DIV) 7, cells were treated with recombinant neuritin (Abcam, Cambridge, UK; 200 ng/ml, dissolved in ddH_2O) or insulin (Sigma Aldrich; 100 nM, dissolved in acidified H_2O). For the kinase- and IR-dependency of neuritin, hippocampal neurons were pretreated with 30 μM KN-62 (Sigma Aldrich), 1 μM Gö6976 (Calbiochem, La Jolla, CA, USA), 100 μM HNMPA-$(AM)_3$ (Merck Millipore, MA, USA) or DMSO for 30 min on DIV7 and stimulated with recombinant neuritin for 30 min, or 30 mM KCl for 6 h.

2.5. Preparation of lysates of cultured neurons and hippocampal dentate gyrus (DG) tissue for western blot analysis

Hippocampal cultured neurons and brains were processed as described previously (Ko et al., 2019). Mice were decapitated and hippocampi were collected for Western blotting 12 h after the final behavioral task or the last stressor of the CUS paradigm. Hippocampal cultured neurons and microdissected hippocampal DG tissue were incubated in 1X lysis buffer (Cell Signaling, Danvers, MA, USA) with protease inhibitor cocktail and phosphatase inhibitor cocktail (Sigma Aldrich). Protein was determined with the Bradford Protein Assay (Bio-Rad Laboratories, Hercules, CA, USA). Nuclear and cytosolic extracts were prepared with nuclear extraction buffer [1% Triton X-100, 50 mM Tris-HCl (pH 8.0), 0.4 M NaCl] and cytosolic extraction buffer [0.5% Triton X-100, 50 mM Tris-HCl (pH 8.0)], respectively. Protein extracts were subjected to SDS-PAGE, transferred to PVDF membranes and incubated with antibodies. Primary antibodies were diluted in 1X TBS with 0.1% Tween-20. The antibodies used are given in Table S2. Secondary antibodies were diluted in 1X TBS with 0.1% Tween-20 containing 5% non-fat dry milk, as follows: anti-rabbit IgG conjugated with HRP, anti-mouse IgG conjugated with HRP (Jackson ImmunoResearch, West Grove, PA, USA). Bands were visualized with an ECL detection kit (ECL STAR; Dyne Bio, Seongnam, Korea). The total densitometric value of each band was quantified with ImageJ software (http://rsbweb.nih.gov/ij/), normalized to the corresponding β-actin level, and expressed as fold change relative to the control value.

2.6. Quantitative real-time RT-PCR

Twelve hours after the last stressor of the CUS paradigm or the final behavioral task, mice were rapidly decapitated and tissue was collected for quantitative PCR. RNA was extracted from hippocampal neurons and DG with Trizol reagent (Invitrogen). Reverse transcription was performed with Improm-II (Promega, Madison, WI, USA), 1 μg of total RNA and oligonucleotide-dT primer. Quantitative real-time PCR (qPCR) was performed on a CFX96 Touch™ Real-Time PCR Detection System (Bio-Rad Laboratories, Madison, CA, USA). Primers used are described in Table S1. DNAs were PCR amplified in triplicate in SensiFAST™ SYBR No-Rox mix (Bioline, London, UK). Ct values for each sample were obtained using CFX Manager Software version 3.0 (Bio-Rad Laboratories). The expression of each gene was normalized to β-actin expression. Normalized expression values were averaged, and average fold changes were calculated.

2.7. Luciferase reporter assays

The pCl-neo-*HDAC5*-WT and pCl-neo-*HDAC5*-S/A expression plasmids were used as described previously (Choi et al., 2015). The Dual-Luciferase® Reporter Assay System (Promega) was used.

2.8. Immunocytochemistry

Hippocampal neurons grown on glass coverslips were transfected with a GFP-*HDAC5* fusion construct (GFP-*HDAC5*-WT; Addgene plasmid #32211) using lipofectamine 2000. To assess neurite outgrowth, hippocampal neurons grown on glass coverslips were infected with lenti-shNC-GFP or lenti-sh*Lgi1*-GFP virus. For the rescue experiment, hippocampal neurons were transfected with pGLV3-H1-shNC-GFP + Puro (shNC-GFP) in combination with pLVX-mCherry-N1 (mCherry) or pGLV3-H1-sh*Lgi1*-GFP + Puro (sh*Lgi1*-GFP) in combination with mCherry or pLVX-*Lgi1*-mut-mcherry (*Lgi1*-mut-mCherry). The cells were fixed with 4% (w/v) paraformaldehyde (PFA) for 20 min, washed three times with PBS for 5 min and incubated with 10% (w/v) normal goat serum and 0.3% Triton X-100 in PBS for 1 h, followed by anti-GFP antibody (Roche Applied Science, Mannheim, Germany) or anti-mCherry antibody (ThermoFisher, MA, USA) in PBS with 10% (w/v) normal goat serum overnight. Next day, the cells were incubated in PBS containing 1% normal goat serum and alexa488-conjugated secondary antibodies (Invitrogen) or Cy3-conjugated secondary antibody (Jackson ImmunoResearch) for 2 h, washed three times with PBS for 5 min and mounted in Vectashield mounting medium containing DAPI (Vector Laboratories Inc., Burlingame, CA, USA). Images were captured with a Delta Vision system (GE Healthcare, Pittsburgh, PA, USA), fluorescence microscope (Nikon, Tokyo, Japan) and confocal microscope (Leica Microsystem, Wetzlar, Germany).

2.9. Measurement of neurite outgrowth

The lengths of GFP^+ and GFP^+/$mCherry^+$ neurites were measured from the soma to the tip of the longest branch with Image J. For Sholl analysis, a series of concentric circles (10 μm intervals) were drawn around the soma of GFP^+ cells, and the intersections of dendrites with each circle were counted. Experiments were performed using four independent cultures, each of which consisted of neurons derived from a separate pregnant mouse. After immunostaining, fields for imaging on coverslips were randomly selected and neurite outgrowth was analyzed.

2.10. Immunohistochemistry

Brain sections from mice were processed for immunohistochemistry as described previously (Ko et al., 2019). Brains were perfused 12 h after the last stressor of the CUS paradigm or the last behavioral tests. Mice were perfused with 4% (w/v) PFA in PBS. Brains were placed in 4% PFA overnight and stored in 30% (w/v) sucrose in PBS at 4 °C. Brain coronal sections (25 μm/section) were cut through the entire anteroposterior extension of the hippocampus and stored in 50% (w/v) glycerol in PBS at −20 °C. For immunostaining GFP or mCherry, brain sections were washed three times with PBS for 5 min, incubated with 5% (w/v) normal goat serum and 0.1% Triton X-100 in PBS for 1 h, followed by incubation overnight with anti-GFP antibody or anti-mCherry antibody in 1% (w/v) normal goat serum and 0.1% Triton X-100 in PBS. Next day, the sections were washed three times with 1% normal goat serum in PBS for 15 min and incubated with alexa488-conjugated secondary antibody or Cy3-conjugated secondary antibody in 1% (w/v) normal goat serum in PBS for 2 h. The cells were washed twice with PBS for 15 min and mounted in Vectashield mounting medium containing DAPI. Images were captured with a fluorescence microscope (Nikon).

2.11. Lentivirus vector production

To overexpress neuritin, its coding sequence (NM_153529.2) was synthesized and subcloned into the lentiviral vector-transferred plasmid pLVX-mCherry-N1 (Cat. #632562, Clontech, CA, USA) to generate pLVX-*Nrn1*-IRES-mCherry (Cosmogenetech, Korea). To silence LGI1, shRNAs were cloned into the pGLV3-H1-GFP + Puro lentiviral vector (Genepharma, China). Their sequences were as follows: negative control shRNA (shNC), 5′-GTTCTCCGAACGTGTCACGT-3’; *Lgi1* shRNA (sh*Lgi1*)-#1, 5′-GCAGCAGAAGGATGGGAAATG-3′ *Lgi1* shRNA (sh*Lgi1*)-#2, 5′-GCCCACCGGAATATAAGAAAC-3’; *Lgi1* shRNA (sh*Lgi1*)-#3, 5′-GGTGTGCAAGCCCATAGTTAT-3’; *Lgi1* shRNA (sh*Lgi1*)-#4, 5′-GCAAAGCAACACAGCTATTCA-3’. Lipofectamine 3000 (Invitrogen) was used to transfect pLVX-mCherry-N1, pLVX-*Nrn1*-IRES-mCherry, pGLV3-H1-shNC-GFP + Puro, and pGLV3-H1-sh*Lgi1*-GFP + Puro along with the packaging vectors psPAX2 and pMD2.G into HEK293T cells to produce the lentivirus.

2.12. Generation of the Lgi1 (Lgi1-WT) and shRNA-resistant Lgi1 (Lgi1-mut) expression vectors

The mouse *Lgi1* coding sequence was amplified by PCR from the cDNA of E18.5 mouse brains with the following primers (F, 5′-GATCTCGAGCTCAAGCCTCGGCCACCATGGAATCAGAAAGCAGC-3’; R, 5′-CGCGGTACCGTCGACTGCAGTGCGCTTAAGTCAACTATG-3′), and subcloned into pLVX-mCherry-N1 vector. For the rescue experiment, shRNA-resistant *Lgi1* (*Lgi1*-mut) was generated by site-directed mutagenesis with the following primers (F, 5′- GTCCACTGTGGTGTGCAAACCTATCGTGATTGACACTCAGCTCTAT-3’; R, 5′-ATAGAGCTGAGTGTCAATCACGATAGGTTTGCACACCACAGTGGAC-3′) and the sequence was confirmed by Sanger sequencing. The target sequence of sh*Lgi1*#4, 5′-GGTGTGCAAGCCCATAGTTAT-3′, was changed to 5′-GGTGTGCAAACCTATCGTGAT-3’. Lipofectamine 3000 (Invitrogen) was used to transfect pLVX-*Lgi1*-mut-mCherry along with the packaging vectors psPAX2 and pMD2.G into HEK293T cells to produce the lentivirus.

2.13. Virus-mediated gene transfer

Mice were anesthetized with a mixture of Rompun (8.5 mg/kg) and Zoletil (17 mg/kg). Stereotaxic surgery were conducted as described previously (Ko et al., 2019). Three microliters of lentivirus were injected bilaterally into each DG of the dorsal hippocampus at a rate of 0.15 μl/min (stereotaxic coordinates in millimeters with reference to the bregma: anteroposterior, −2.0; mediolateral, ±1.5; dorsoventral, −2.4) using a 26s gauge syringe (Hamilton).

2.14. Chromatin immunoprecipitation (ChIP) assays

Hippocampal primary neurons (DIV4) were transfected with Myc-*HDAC5* using lipofectamine 2000 reagent (Invitrogen). Neurons and tissues were fixed with 18.5% (w/v) paraformaldehyde in PBS and sonicated. The sonicated samples were rotated with protein A agarose (Roche Applied Sciences) for 1 h at 4 °C to preclear them. Antibodies were added to the sonicated samples and incubated overnight at 4 °C. The antibodies used are given in Table S2. Immunoprecipitated DNA samples were dissolved in distilled H_20 and used for real-time PCR (CFX96 Touch Real-Time PCR Detection System, Bio-Rad). Input and immunoprecipitated DNAs were PCR amplified in triplicate in Sensi-FAST™ SYBR No-Rox mix (Bioline).

2.15. Immunoprecipitation (IP)

IP was performed as described previously (Ko et al., 2019). To confirm binding of HDAC5 to the MEF2D, hippocampal primary neurons (DIV4) were transfected with Myc-*HDAC5* using lipofectamine 2000. Myc-*HDAC5* was immunoprecipitated from Myc-*HDAC5*- transfected neurons using anti-Myc monoclonal antibody (Abm, BC, Canada). To confirm binding of neuritin to the IR, hippocampal primary neurons (DIV4) were transfected with pIRES-EGFP or pIRES-Flag-*Nrn1*-EGFP (Flag-*Nrn1*) using lipofectamine 2000. pIRES-EGFP and Flag-*Nrn1* plasmids have been described previously (An et al., 2014). FLAG-neuritin was immunoprecipitated from Flag-*Nrn1*-transfected neurons using anti-FLAG monoclonal antibody (Sigma Aldrich).

2.16. Mef2d siRNA

Control siRNA (SC-37007, Santa Cruz, TX, USA) and *Mef2d* siRNA (SC-38065, Santa Cruz) were solubilized in RNAse-free water. Hippocampal primary neurons were transfected with control siRNA or *Mef2d* siRNA using lipofectamine RNAiMAX reagent (Invitrogen).

2.17. Drug administration

Fluoxetine (Tocris Bioscience, Bristol, UK) was solubilized in saline and administered intraperitoneally (i.p.) to mice at 10 mg/kg/d for 3 wks. For fluoxetine treatment, animals were first exposed to CUS (7 days) and then administered fluoxetine or saline for 21 days with continued CUS, starting on day 8 of CUS. Serum fluoxetine levels for the 10 mg/kg/day (i.p.) dose in rodents are towards the middle range of plasma levels (100–700 ng/ml) found in patients taking 20–80 mg/day Prozac (Koran et al., 1996; Perrone et al., 2004).

2.18. Chronic unpredictable stress (CUS) procedure

CUS experiments were performed as described previously (Koo et al., 2010). Mice were exposed to two or three stressors per day for 28 days. The CUS procedure is summarized in Table S3.

2.19. Behavioral experiments

Behavioral experiments were performed according to the previously published protocol (Ko et al., 2019; Rudyk et al., 2019) with minor modifications. They were conducted in the following order, from least stressful to most stressful, starting on day 27 after CUS: LMA, SCT, NSFT, FST and LHT. Mice were tested for home cage locomotor activity, as well as sucrose consumption behavior on days 27–28 of the CUS procedure. At the termination of stress, behavioral tests as described below were conducted to evaluate signs of behavioral despair (using NSFT, FST and LHT) starting on post-stress days 29–31. Animals were tested in random order during the dark cycle. Mice were transferred to the testing room 2 h before testing, and acclimated to room conditions. After each test session, the apparatus was cleaned with 70% alcohol to remove any odor and trace of the previously tested mouse.

2.19.1. Locomotor activity test (LMA)

Mice were placed in a white box (50 × 50 × 20 cm) and their distances moved in 5 min were recorded by web camera (HD310, Logitech, Switzerland). Recorded data were analyzed with an ANY-maze video tracking system (Stoelting Co., Wood Dale, IL, USA).

2.19.2. Sucrose consumption test (SCT)

The SCT was performed in the home cage. Mice were exposed to 2% (w/v) sucrose solution for 48 h and the sucrose was removed for 12 h. After 12 h, the mice were again exposed to sucrose solution for 1 h and the amount of sucrose solution consumed was measured.

2.19.3. Novelty suppressed feeding test (NSFT)

Mice were deprived of food for 1 d before the test. The amount of time that the mice spent eating was measured after placing three feeds in the center of a white box (50 × 50 × 20 cm) in a lightless space.

2.19.4. Forced swimming test (FST)

Mice were placed in a 24 °C water-filled transparent acryl cylinder (height 30 cm, diameter 15 cm) and recorded for 6 min with a video camera recorder (HDR-PJ230, Sony, Japan). Immobility time was scored during the last 4 min.

2.19.5. Learned helplessness test (LHT)

LHT was conducted as previously described (Duman et al., 2007). LHT consists of inescapable shock training (day 1) and active avoidance testing (day 2). On the first day (day 1), mice were exposed to inescapable shock (180 footshocks, 0.3 mA, shock amplitude, 4-sec duration, 30-sec average interval) in one side of the shuttle box. On the second day (day 2), they were exposed to 30 escape trials (0.3 mA footshocks, 25-sec duration, 30-sec average interval). The shuttle box's door was then opened for 25-sec and the mice were free to run to the other side of the shuttle box before the door closed. Latency to escape was recorded with Gemini avoidance system software. Latencies to escape over first 10 escape trials or total escape trials were analyzed.

2.20. Statistical analysis

Student's *t*-test was used for comparing pairs of groups when measuring biochemical parameters. Statistical differences between sets of four groups in behavioral experiments were analyzed by one-way or two-way ANOVA, followed by multiple comparison analysis including Bonferroni, Newman-Keuls or LSD tests (GraphPad Prism 7.04, GraphPad software). Unpaired two-tailed Student's *t*-test was used for multiple comparisons between groups when assessing the effects of genotype and the effects of lenti-shRNA infusion. When the measurement variable is not normally distributed, results were analyzed by Kruskal Wallis test, a *non-parametric* equivalent of two-way ANOVA and followed by Dunn's test. Kolmogorov-Smirnov (K–S) test was used to compare the cumulative mEPSC frequency and amplitude between groups. All experiments were carried out at least three times. The results are presented as mean ± SEM. Statistical significance was set at $p < 0.05$ in two-tailed tests. Related statistical parameters are specified in Table S4.

3. Results

3.1. LGI1 expression inhibited by exposure to CUS, but promoted by neuritin

To probe the molecular mechanisms by which neuritin prevents the atrophy of neurites in mice being exposed to CUS, we identified potential target genes that are affected in common by neuritin treatment and CUS. Of the various transcription factors, the myocyte-enhancer factor 2 family (MEF2) seems to be important for neurite outgrowth and synaptic remodeling (Flavell et al., 2006; Lin et al., 1996; Potthoff and Olson, 2007). We first examined the effects of CUS involving prolonged exposure to either physical or psychological stressors on several possible downstream targets of MEF2, including *Arc, Klf4, Klf6, Klf9, C-fos, Nr4a1, Egr1* and *Lgi1* (Fig. 1A and S1A), which have been previously reported to be involved in neurite outgrowth- and neuroplasticity-related synaptic alterations (Flavell et al., 2008). LGI1 has almost the same localization pattern across pre- and post-synaptic neurons in the hippocampus; it has similar functions to neuritin, and both regulate neuronal excitability through expression of the outward potassium current (I_A) subunit (Carrasquillo et al., 2012; Yao et al., 2016), and glutamatergic transmission (Boillot et al., 2016). CUS reduced the mRNA and protein levels of LGI1 in the hippocampal DG of mice (Fig. 1A and B), a subregion that is reduced in volume in major depressive disorder (MDD) (Malykhin and Coupland, 2015). The downregulation of LGI1 after CUS was rescued by fluoxetine treatment for 3 weeks, suggesting that LGI1 is responsible at least in part for the antidepressant effects (Fig. 1B). This is in line with our previous findings that neuritin mRNA levels were reduced in subregions of the dorsal hippocampus of chronically stressed mice including the DG granule cell layers, and reversed by chronic administration of fluoxetine (Son et al., 2012). Given the similarity of localization and function, these results suggest that the extent of neuritin induction in the hippocampus may be linked to LGI1 expression.

Since LGI1 is required for maturation of the synapses of postsynaptic neurons (Lovero et al., 2015), we surmised that it might be required for neuritin-dependent neurite outgrowth and axonal branch formation. We found that soluble neuritin induced levels of *Arc, Klf4, C-fos, Nr4a1, Egr1*

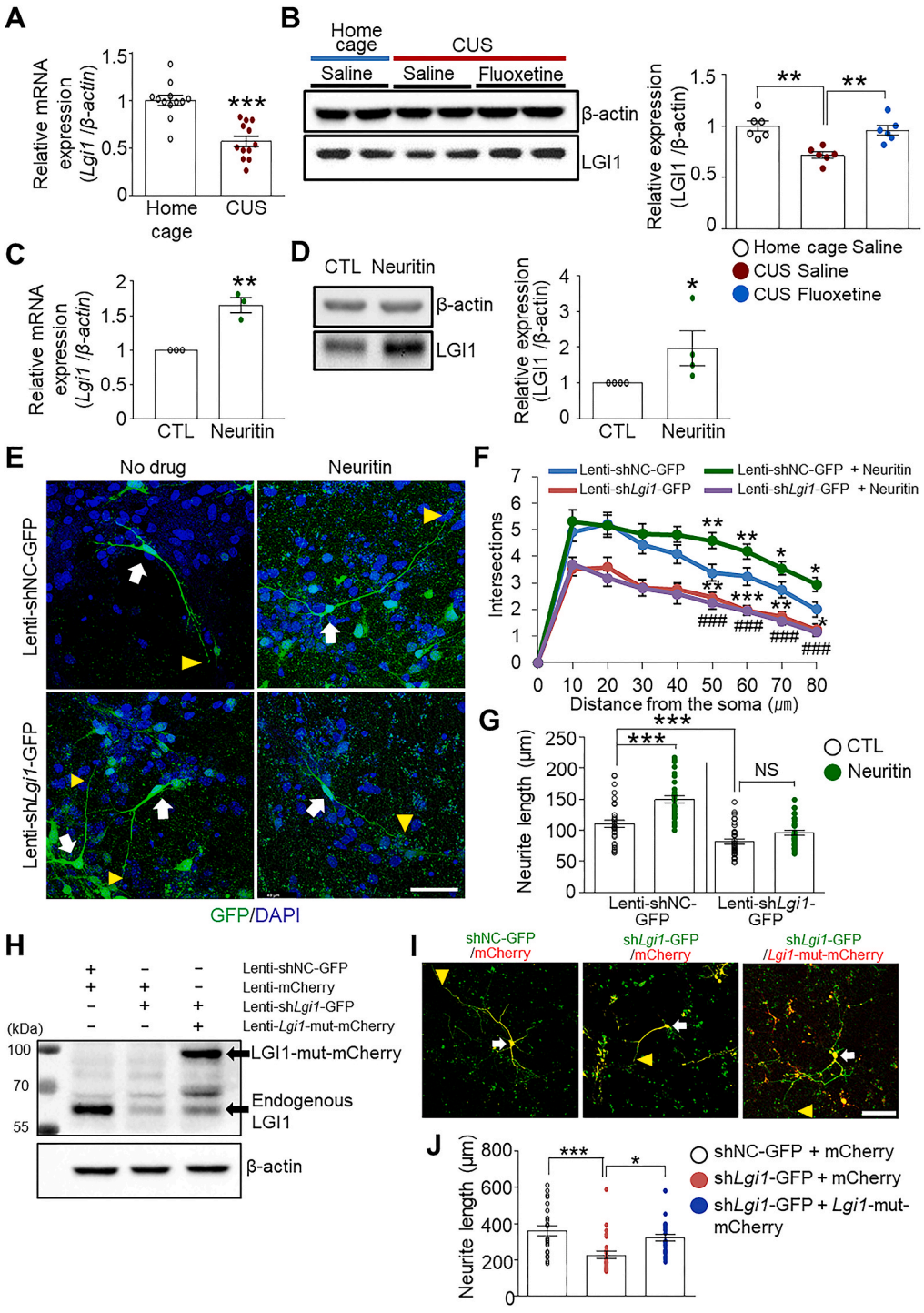

Fig. 1. CUS downregulates LGI1 expression, while soluble recombinant neuritin induces it. (A) Mice were exposed to CUS for 28 d and decapitated 5 min after the last stressor. *Lgi1* mRNA levels in the hippocampal DG ($n = 12$ per group). (B) Mice exposed to CUS were injected with fluoxetine (10 mg/kg) or saline daily for 21 d starting on day 8. Immunoblots of LGI1 using protein extracts of the hippocampal DG ($n = 6$ per group). (C) Hippocampal neurons (DIV7) were treated with soluble neuritin at 200 ng/ml for 6 h and *Lgi1* mRNA levels were measured by real-time PCR ($n = 3$ per group). (D) Representative immunoblots of hippocampal neurons treated with soluble neuritin (200 ng/ml) for 6 h. Quantitative data for LGI1 expression ($n = 4$). (E) Representative images of GFP(+) hippocampal neurons. After confirming effective knockdown by lenti-sh*Lgi1*-GFP (Fig. S2), neurons (DIV4) were pretreated with lenti-shNC-GFP or lenti-sh*Lgi1*-GFP and stimulated with soluble neuritin (200 ng/ml) for 3 d (Scale bar, 50 μm). (F) Sholl analysis of all orders of branching. ($n = 33$–34 neurons per conditions from four independent cultures). (G) Length of neurites. ($n = 33$–37 neurons per conditions from four independent cultures). (H) Verification for specificity of the sh*Lgi1* by Western blotting. Neurons were infected with lenti-shNC-GFP or lenti-sh*Lgi1*-GFP in the presence of either lenti-mCherry or lenti-*Lgi1*-mut-mCherry. (I, J) Transfection of neurons with sh*Lgi1*-GFP and *Lgi1*-mut-mCherry constructs. ($n = 28$–30 neurons per conditions from four independent cultures; Scale bar, 100 μm). Data were obtained from four independent cultures, each of which consisted of neurons derived from a separate pregnant mouse (E–J). White arrow: soma; yellow arrowhead: end point of neurites. In (A)–(H), Data are represented as mean ± SEM; $^{*}p < 0.05$, $^{**}p < 0.01$, $^{***}p < 0.001$ compared with home cage (A) or CTL (C and D) or lenti-shNC-GFP (F), $^{\#\#\#}p < 0.001$ compared with lenti-shNC-GFP + neuritin. Immunoblots were normalized to the level of β-actin which was used as home cage-saline (B) or CTL (D). Statistics: Unpaired two-tailed *t*-test (A). Student's *t*-test (C and D). One-way ANOVA (B and J) or two-way ANOVA (F and G) followed by Bonferroni posttest. Statistics are detailed in Table S4. (For interpretation of the references to colour in this figure legend, the reader is referred to the Web version of this article.)

and *Lgi1* mRNAs in hippocampal neuronal cultures (Fig. 1C and S1B). An increase in *Lgi1* mRNA became obvious after 1 h treatment of neuritin, and was maximal (~2-fold) after 24 h (Fig. S1C). An increase of LGI1 protein became apparent after 6 h of treatment (Fig. 1D). We next investigated the effects of LGI1 on neuritin-induced neuritogenesis by delivering lentiviral vector-mediated constructs encoding short-hairpin *Lgi1* RNA (lenti-sh*Lgi1*) along with recombinant neuritin. The efficacies of three shRNA sequences were compared in vitro (Fig. S2) and shRNA#3 was used in subsequent experiments. Infusion of neurons with GFP-tagged lenti-sh*Lgi1* (lenti-sh*Lgi1*-GFP) stably knocked down LGI1 expression by ~ 50% in mouse hippocampal neurons (Fig. S2) and dramatically decreased the number of distal branches and the length of neurites measured by Sholl analysis (Fig. 1E, F and G). Soluble neuritin significantly increased the number of distal branches at 50–80 μm distance from the soma (Fig. 1E and F), as well as the length of primary dendrites (Fig. 1E and G). These neuritin-induced effects were blocked by prior introduction of lenti-sh*Lgi1*-GFP (Fig. 1E-G). To confirm the specificity of the shRNA-mediated knockdown, we introduced into sh*Lgi1*-GFP cells empty vector (lenti-mCherry) and shRNA-resistant *Lgi1* (lenti-*Lgi1*-mut-mCherry), which has silent mutations that make it resistant to the shRNA sequence. Western blots of these cells showed that while the endogeneous *Lgi1* was silenced by the lenti-sh*Lgi1*-GFP, the co-expressed shRNA-resistant mutant *Lgi1* was robustly expressed in the lenti-sh*Lgi1*-GFP-transduced cells (Fig. 1H). As observed in the neurite length assays, introduction of the shRNA-resistant *Lgi1*--mut-mCherry reversed the inhibition of neurite outgrowth in neurons expressing sh*Lgi1*-GFP, thus excluding possible off-target effects of the shRNA (Fig. 1I and J). These results are in agreement with our previous work showing that neuritin induces neurite outgrowth (Son et al., 2012), and indicates that LGI1 is implicated in the neuritin-mediated alteration of neuronal morphology.

3.2. Neuritin-induced expression of LGI1 through HDAC5 phosphorylation and MEF2D-mediated transcription

To identify the molecular mechanisms by which neuritin induces LGI1, we investigated potential signaling pathways for LGI1 expression. MEF2 transcriptional activity is repressed by interaction with histone deacetylase 5 (HDAC5) in the nucleus. Phosphorylated HDAC5 is exported to the cytoplasm, leading to activation of MEF2 target genes (Guise et al., 2014; McKinsey et al., 2000a), which may generate behavioral plasticity (Barbosa et al., 2008). Therefore, we investigated whether neuritin could elicit HDAC5 phosphorylation, using antibodies to phospho-Ser259 and Ser498 HDAC5, respectively. Incubation of hippocampal neurons with recombinant neuritin stimulated phosphorylation of HDAC5 at Ser259/498, which reached peak levels at 200 ng/ml (Fig. 2A). The effect of neuritin (200 ng/ml) on HDAC5 phosphorylation was time-dependent and peaked after approximately 30 min (Fig. S3A).

To determine whether neuritin-induced HDAC5 phosphorylation was mediated by Ca^{2+}/calmodulin-dependent kinase II (CaMKII) and protein kinase D (PKD), two kinases previously shown to phosphorylate HDAC5 in cultured hippocampal neurons (McKinsey et al., 2000b; Vega et al., 2004), we used KN-62, a CaMKII inhibitor, and Gö6976, a PKD

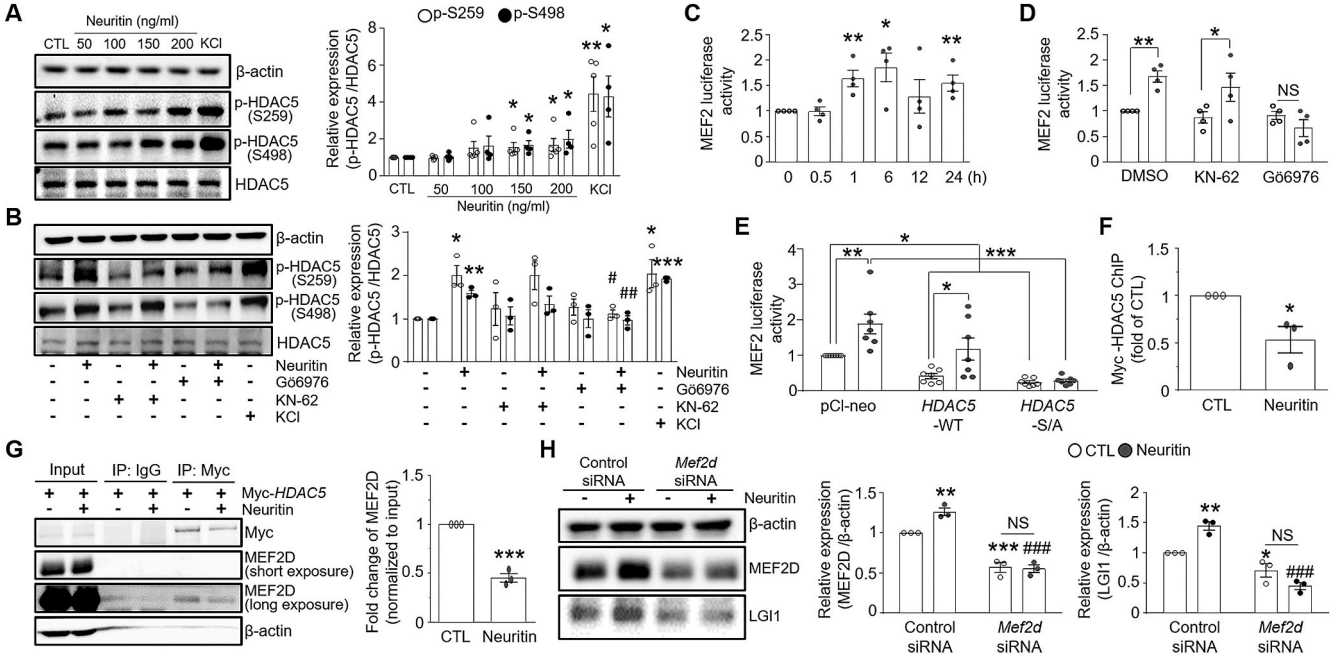

Fig. 2. Neuritin induces LGI1 expression through HDAC5 phosphorylation and MEF2D-mediated transcription. (A) Representative immunoblots of p-HDAC5 in hippocampal neurons (DIV7) treated with various concentrations of recombinant soluble neuritin for 30 min or with KCl (30 mM) for 6 h (n = 4–5). (B) Representative immunoblots of p-HDAC5 from hippocampal neurons pretreated with KN-62 (30 μM) or Gö6976 (1 μM) for 30 min and incubated with soluble neuritin or KCl (n = 3). (C–E) Luciferase assays. MEF2-luciferase activity was normalized with Renilla luciferase activity and is depicted relative to the control (CTL), and expressed as fold change relative to the CTL. (C) Mouse hippocampal neurons (DIV4) transfected with pGL3-Luc and pGL3-MEF2-Luc were treated with neuritin for the indicated times (n = 4). (D) Mouse hippocampal neurons transfected with pGL3-Luc and PGL3-*MEF2*-Luc were treated with neuritin in the presence of KN-62 or Gö6976 (n = 4). (E) Neurons transfected with pGL3-Luc, pGL3-*MEF2*-Luc, pCl-neo, pCl-neo-*HDAC5*-WT or pCl-neo-*HDAC5*-S/A were treated with recombinant soluble neuritin for 1 h (n = 7). (F) ChIP assays. Binding of HDAC5 to the *Lgi1* promoter was decreased in recombinant soluble neuritin-treated mouse hippocampal neurons (n = 3). (G) IP. Neurons (DIV4) transfected with Myc-*HDAC5* were treated with recombinant soluble neuritin (200 ng/ml) for 1 h. Binding of HDAC5 to MEF2D in mouse hippocampal neurons was decreased by recombinant soluble neuritin treatment (n = 3). (H) Neurons (DIV4) transfected with control siRNA and *Mef2d* siRNA were treated with recombinant soluble neuritin (200 ng/ml) for 6 h. Representative immunoblots *(Left)* and quantitative data *(Right)* for MEF2D or LGI1 protein expression (n = 3). In (A)–(H), Data are represented as mean ± SEM; $^{*}p < 0.05$, $^{**}p < 0.01$, $^{***}p < 0.001$ compared with CTL, $^{\#}p < 0.05$, $^{\#\#\#}p < 0.001$ compared with recombinant soluble neuritin treatment. Statistics: Student's t-test (A, C, F and G). One-way ANOVA (B) or two-way ANOVA (D) followed by LSD posttest. Two-way ANOVA followed by Newman-Keuls posttest (E) or Bonferroni posttest (H). Statistics detailed in Table S4.

inhibitor. Indeed, neuritin-induced HDAC5 phosphorylation was attenuated by Gö6976, but not by KN-62 (Fig. 2B), indicating that neuritin induces HDAC5 phosphorylation mainly via PKD. In line with this, neuritin, like HDAC5, induced progressive phosphorylation of PKD (Fig. S3B). Nuclear export of HDAC5 is dependent on phosphorylation of Ser259/498 (Chang et al., 2013). As expected, neuritin increased HDAC5 phosphorylation in cytoplasmic fractions and reduced nuclear HDAC5 (Figs. S4A and S4B). Neuritin-induced cytoplasmic translocation of HDAC5 was time-dependent, reaching a maximum after 30 min, and was maintained for 24 h (Figs. S4C and S4D). These results suggest that neuritin reduces HDAC5 repression of MEF2-driven *Lgi1* transcription.

Given the capability of neuritin to phosphorylate HDAC5, neuritin would induce LGI1 expression through increased MEF2 binding to a sequence located approximately 180 bp upstream of the transcription start site of *Lgi1* (Andres et al., 1995; Lyons et al., 1995). We observed in MEF2 luciferase reporter assays that MEF2-luciferase activity was significantly elevated after 1 h of treatment with neuritin and remained elevated for 24 h (Fig. 2C). Neuritin-induced MEF2-luciferase activity was suppressed by Gö6976, but not by KN-62 (Fig. 2D), supporting that neuritin-mediated HDAC5 phosphorylation is PKD-dependent. MEF2 activity completely failed to be activated by pCl-*HDAC5*-S/A, a mutant form of HDAC5 in which Ser259/498 are mutated to alanines (Fig. 2E), indicating that neuritin-induced phosphorylation of HDAC5 is a prerequisite for neuritin-induced MEF2 transcriptional activity.

To directly assess whether neuritin-induced MEF2 activity plays a role in LGI1 expression, binding of myc-HDAC5 to the putative binding site of MEF2 in the promoter region of *Lgi1* was analyzed by chromatin immunoprecipitation (ChIP) assays. Recombinant neuritin significantly reduced the amount of HDAC5 protein in the promoter region of *Lgi1* (Fig. 2F), thus confirming that neuritin increases expression of LGI1 by reducing HDAC5 repression. Notably, recombinant neuritin markedly increased *Mef2d* mRNA, whereas it only increased expression of *Mef2a* and *c* mRNAs to a moderate extent (Fig. S4E), suggesting that MEF2D plays a critical role in inducing LGI1 expression. Neuritin also decreased HDAC5-MEF2D protein complexes, as demonstrated by co-immunoprecipitation, suggesting that neuritin derepresses MEF2D

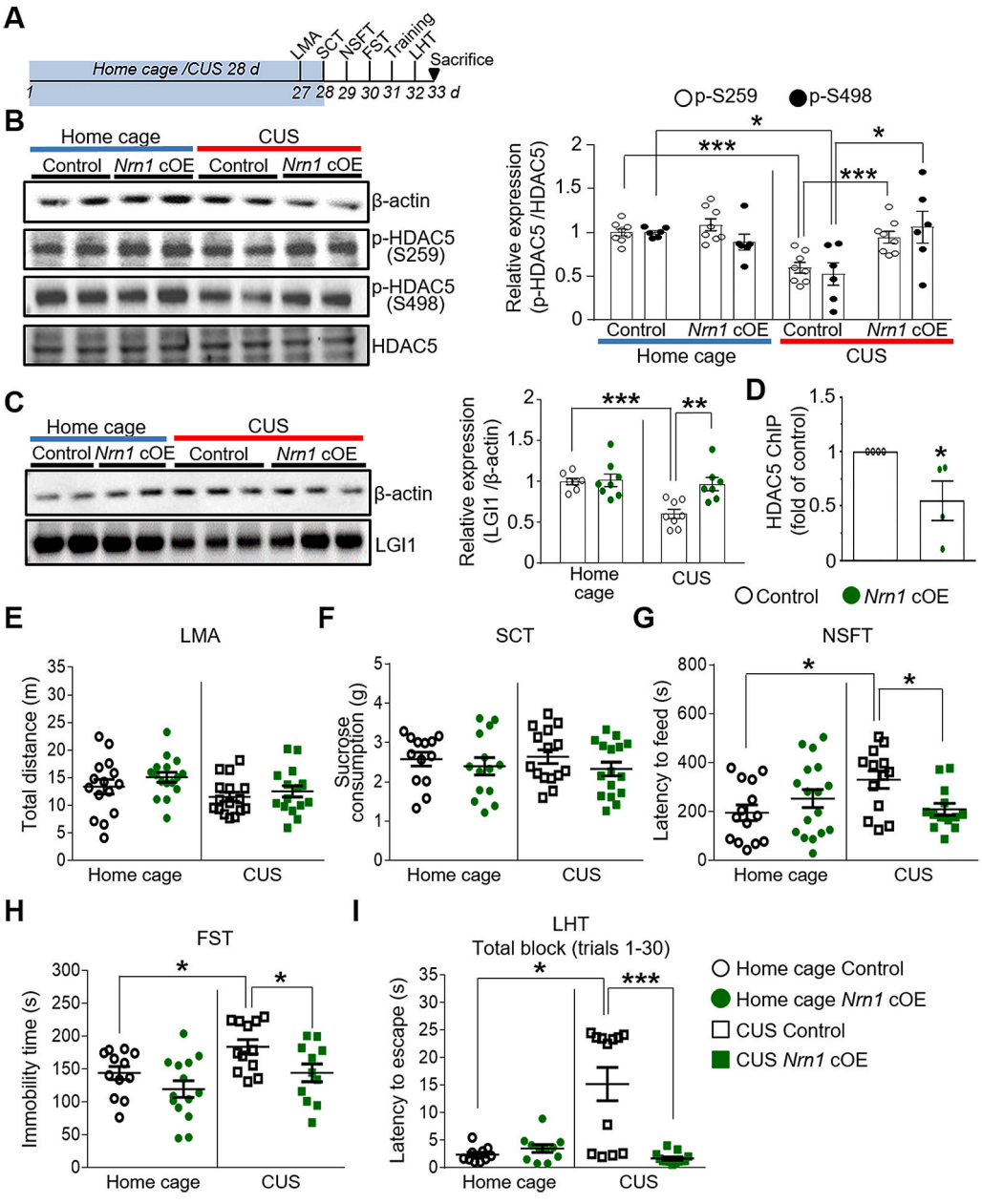

Fig. 3. *Nrn1* cOE mice produce increases in LGI1 in the hippocampal DG and display antidepressant-like behaviors under CUS. (A) Timeline of the experimental procedures. Mice were exposed to CUS for 28 d. (B) Immunoblots of p-HDAC5 using protein extracts of the hippocampal DG (*Left*) (n = 6–8 per group). (C) Immunoblots of LGI1 using protein extracts of the hippocampal DG (n = 7–8 per group). (D) ChIP assay. Binding of HDAC5 to the *Lgi1* promoter decreased in the hippocampus of *Nrn1* cOE mice under CUS (n = 4 per group). (E) LMA. Total distance (n = 15–16 per group). (F) SCT. Total sucrose consumption (n = 13–16 per group). (G) NSFT. *Nrn1* cOE mice showed a decrease in latency to feed compared with littermate controls under CUS (n = 13–17). (H) FST. *Nrn1* cOE mice displayed a decrease in immobility compared with littermate controls under CUS (n = 11–14 per group). (I) LHT. *Nrn1* cOE mice showed a decrease in latency to escape compared with control mice under CUS (n = 10–13 per group). In (B)–(I), Data are represented as mean ± SEM; $^{*}p < 0.05$, $^{**}p < 0.01$, $^{***}p < 0.001$. Statistics: Two-way ANOVA followed by Bonferroni post-test (B, C and G). Unpaired two-tailed *t*-test (D, H). Kruskal Wallis test followed by Dunn's test (I). Statistics detailed in Table S4.

transcriptional activity (Fig. 2G). Consistently, *Mef2d* siRNA completely blocked neuritin-induced expression of LGI1, indicating that MEF2D was responsible for neuritin-induced LGI1 expression (Fig. 2H).

3.3. Increases in LGI1 expression and resilience to stress in neuritin cOE (conditionally overexpressing) mice

The finding that addition of exogenous neuritin to cultured hippocampal neurons led to a two-fold increase in LGI1 expression (Fig. 1D) prompted us to investigate whether neuritin expression *in vivo* resulted in HDAC5 phosphorylation and MEF2-driven stimulation of LGI1 expression comparable to that caused by soluble neuritin. To further determine the role of neuritin in the hippocampus, and to extend our previous study, we generated *Nrn1*$^{flox/flox}$ mice and crossed them with *Pomc-cre* mice generating *Nrn1*$^{flox/flox}$*;Pomc-cre* (*Nrn1* cOE) progeny in which expression of *Nrn1* mRNA in the granule cells of the DG was 2–4 fold higher than in littermate controls (control; *Nrn1* $^{flox/flox}$) (Fig. S5D). Neuritin protein levels were also strongly increased in hippocampal DG neurons (Fig. S5E). Initially, we employed biochemical approaches to examine the cellular and molecular consequences of neuritin overexpression *in vivo* (Fig. 3). Western blot analysis revealed no significant effect on either the proportion of p-HDAC5 relative to total HDAC5 or on LGI1 expression in the hippocampal DGs of *Nrn1* cOE mice compared to the *Nrn1* $^{flox/flox}$ (control) mice in the home caged (control) group (Fig. 3B and C). CUS reduced the proportion of p-HDAC5 in the control mice, in agreement with previous results (Choi et al., 2017). The CUS-mediated reductions in p-HDAC5 were rescued in the *Nrn1* cOE mice (Fig. 3B). In addition, the LGI1 levels induced by CUS were reversed in the *Nrn1* cOE mice (Fig. 3C), and fewer HDAC5-MEF2 protein complexes were bound to the *Lgi1* promoter in the hippocampi of *Nrn1* cOE mice under CUS (Fig. 3D). These results indicate that neuritin exert its action via HDAC5-LGI1 signaling.

We previously reported that virus-mediated overexpression of neuritin in the hippocampal DG has antidepressant-like effects while stimulating neurite outgrowth. The antidepressant-like effects of neuritin are prominent under CUS (Son et al., 2012). As we had detected MEF2-driven LGI1 expression in the granule neurons of *Nrn1* cOE mice, we asked if neuritin-mediated LGI1 expression in hippocampal cells contributed to its antidepressant-like effects. We first investigated whether the stress-induced behaviors were affected in *Nrn1* cOE mice, as indicated by responsiveness in the novelty-suppressed-feeding test (NSFT), forced swim test (FST) and learned helplessness test (LHT), which have been widely used to assess behavioral despair (Fig. 3G-I). Under non-stress conditions, no differences were observed between *Nrn1* cOE and littermate controls in any of the behavioral tests for depression-like behaviors (Fig. 3G-I). However, littermate controls exposed to CUS exhibited significantly more immobility in the FST than *Nrn1* cOE mice, which had similar immobility times to those of mice tested under ‘‘non-stress’’ conditions. This behavior is interpreted as decreased depression-like behavior or increased coping-like behavior (Fig. 3H). In agreement with this, only the control mice had an increase in latency to feed in the NSFT, and to escape in the LHT (Fig. 3I). No difference between *Nrn1* cOE mice and controls was observed in the locomotor activity test (LMA) and in sucrose consumption, indicative of stress-induced anhedonia (Fig. 3E and F). Taken together our observations indicate that *Nrn1* cOE mice are normal in the absence of stress and are resilient to CUS-induced behavioral deficits.

Since both neuritin and LGI1 are implicated in synaptic transmission (An et al., 2014; Fukata et al., 2006, 2010), we examined spontaneous miniature excitatory postsynaptic currents (mEPSCs) and found that the amplitudes and frequencies of mEPSCs were comparable between genotypes in the home caged group. However, the frequencies, but not amplitudes, of mEPSCs were significantly higher in neurons from *Nrn1* cOE mice than in those from control mice in CUS (Fig. S6), indicative of enhanced synaptic transmission, and supporting the view that neuritin produces stress resilience. The mEPSC amplitudes were significantly higher in neurons from the CUS group than in those from home caged group both in control and *Nrn1* cOE mice (Fig. S6), in line with that corticosterone enhances mEPSC amplitudes (Martin et al., 2009; Yuen et al., 2009).

To assess whether virus-mediated overexpression of neuritin also has comparable effects to those seen in the *Nrn1* cOE mice, we infused lenti-*Nrn1*-IRES-mCherry (lenti-*Nrn1*-mCherry) into the DG of WT mice (Fig. 4A). mCherry expression was evident in the DG, and *Nrn1* expression was markedly enhanced at the mRNA level at 5 wks post-infusion (Fig. 4B and C). Mice infused with lenti-*Nrn1*-mCherry had lower immobility in non-stressed, home-caged conditions than those infused with lenti-mCherry, suggesting that neuritin has a protective role against stress in the FST (Fig. 4G). Using the CUS approach, we assessed the role of neuritin in chronic stress-induced behaviors. In control mice infused with lenti-mCherry, CUS caused the expected increase in immobility in the FST, and in latency to escape in the LHT, and these effects were prevented by lenti-*Nrn1*-mCherry (Fig. 4G and H). Latency to feed in the NSFT was also lower in those infused with lenti-*Nrn1*-mCherry than in control mice under CUS (Fig. 4F). Together, these results demonstrate that neuritin reduces depression-like behaviors. Under CUS, in mice infused with lenti-*Nrn1*-mCherry the p-HDAC5 and LGI1 levels induced were the reverse of those in mice infused with lenti-mCherry (Fig. 4I–K), consistent with the results seen in the *Nrn1* cOE mice (Fig. 4F–H). These results demonstrate that neuritin overexpression *in vivo,* like exposure to soluble neuritin, increased HDAC5 phosphorylation and LGI1 expression.

3.4. Resilience to CUS in Nrn1 cOE mice is abolished by depleting LGI1

The observation that *Nrn1* cOE mice underwent a reversal of the decrease in LGI1 level induced by CUS led us to examine whether *Nrn1* cOE mice rescued the behavioral responses to stress observed in *Lgi1* knockdown mice (Fig. 5A). To determine the importance of endogenous LGI1 levels in mediating depression-like behaviors and the response to CUS, we established a lentiviral-based system to specifically knock down endogenous *Lgi1* in the DG. When lenti-sh*Lgi1*-GFP was injected into the DG of control and *Nrn1* cOE mice, *Lgi1* expression was markedly reduced at the mRNA level at 5 wks post-infusion (Fig. 5B). Behavioral analysis in the absence of CUS showed that infusion of lenti-sh*Lgi1*-GFP into littermate controls and *Nrn1* cOE mice produced at best a tendency towards anhedonic responses in the sucrose consumption test compared with those infused with lenti-shNC-GFP (Fig. S7C). Infusion of lenti-sh*Lgi1*-GFP into control and *Nrn1* cOE mice also did not have significant effects on behaviors in the NSFT and LHT (Figs. S7D and S7F). However, control mice infused with lenti-sh*Lgi1*-GFP were significantly more immobile compared to lenti-shNC-GFP-injected mice (Fig. S7E), suggesting that endogenous LGI1 levels play a role in mediating depression-like behaviors. Infusion of lenti-sh*Lgi1*-GFP in the DG of *Nrn1* cOE mice, to a lesser extent, increased the immobility. Next, experiments were conducted to determine if knocking down *Lgi1* influenced responses to CUS. Lenti-sh*Lgi1*-GFP infusion did not affect sucrose consumption in either littermate controls or *Nrn1* cOE mice (Fig. 5D). Depletion of LGI1 did not further affect behaviors in the littermate control mice (Fig. 5E-G). In contrast, the stress resilience observed in *Nrn1* cOE mice in the NSFT, FST and LHT was prevented by *Lgi1* knockdown (Fig. 5E-G). No behavioral changes were observed in the LMA (Fig. 5C). Together, these results indicate that LGI1 is required at least in part for the behavioral resilience seen in stressed *Nrn1* cOE mice, and suggest that LGI1 plays a role in protection against stress-induced behavioral responses in a neuritin-mediated signaling pathway.

3.5. Neuritin-mediated expression of LGI1 dependent on insulin receptors

We attempted to identify the upstream signals involved in LGI1 expression. Previous studies have reported that neuritin acts on insulin receptors (Yao et al., 2016), which are tyrosine kinase-coupled receptors

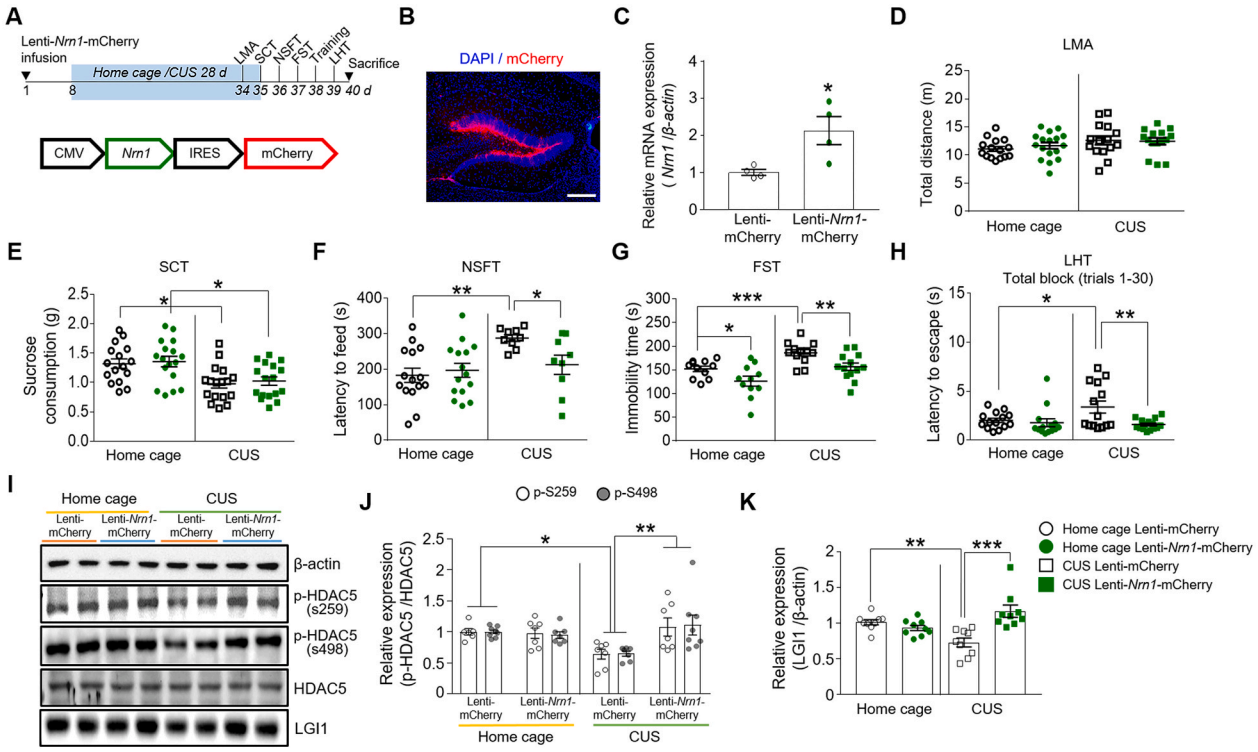

Fig. 4. Overexpression of neuritin in the hippocampal DG mimics the phenotype of *Nrn1* cOE mice. (A) Timeline of the experimental procedures. Mice were injected with lenti-mCherry and lenti-*Nrn1*-mCherry and exposed to CUS for 28 d starting on day 8. (B) Localization of the lentivirus in the hippocampal DG by mCherry staining (scale bar, 200 μm). (C) *Nrn1* mRNA measured by real-time PCR ($n = 4$). (D) LMA. Total distance ($n = 15$–17 per group). (E) SCT. Total sucrose consumption ($n = 16$–17 per group). (F) NSFT. Lenti-*Nrn1*-mCherry-injected mice displayed a decrease in latency to feed compared with lenti-mCherry-injected mice under CUS ($n = 9$–15 per group). (G) FST. Lenti-*Nrn1*-mCherry-injected mice displayed a decrease in immobility compared with lenti-mCherry-injected mice ($n = 11$–13 per group). (H) LHT. Lenti-*Nrn1*-mCherry-injected mice showed a decrease in latency to escape compared with lenti-mCherry-injected mice under CUS ($n = 14$–15 per group). (I and J) Immunoblots of p-HDAC5 using protein extracts of hippocampal DG (S259: $n = 6$–7 per group, S498: $n = 7$–8 per group). (I and K) Immunoblots of LGI1 ($n = 9$ per group). In (C)–(K), Data are represented as mean ± SEM; $^{*}p < 0.05$, $^{**}p < 0.01$, $^{***}p < 0.001$. Statistics: Unpaired two-tailed *t*-test (C, E and G). Two-way ANOVA followed by Newman-Keuls posttest (F and H) or Bonferroni posttest (J and K). Statistics detailed in Table S4.

(Shimada et al., 2016). To ascertain the effect of neuritin on tyrosine phosphorylation of the insulin receptor (IR), we first followed the phosphorylation of the IR β-subunit (IRβ) and insulin receptor substrate-1 (IRS-1), a downstream effector of IR signaling in response to neuritin. Since administration of neuritin was found to induce p-IRβ and p-IRS1 expression (Fig. 6A), we examined whether blockade of the IRs abolished the neuritin-induced phosphorylation of IRS and HDAC5. Indeed, pretreatment with HNMPA-$(AM)_3$, an insulin receptor inhibitor, did reduce neuritin-mediated phosphorylation of IRS and HDAC5 (Fig. 6B–D). Importantly, it also reduced neuritin-induced LGI1 expression (Fig. 6B and E), which indicates that neuritin acts on LGI1 via IRs. To directly investigate whether neuritin associates with the IRs, we performed co-immunoprecipitation (co-IP) experiments. Cells expressing a FLAG-neuritin construct were subjected to IP using anti-FLAG antibody, and both inputs and co-IP fractions (IP α-FLAG) were immunoblotted with anti-IRβ or anti-FLAG antibodies. The IRβ was found to be co-immunoprecipitated with anti-FLAG antibodies, thus demonstrating neuritin-IR interaction (Fig. 6F). Given that IRs are involved in neuritin signaling, we asked whether insulin induced the phosphorylation of IRS1, PKD and HDAC5 and increased LGI1 protein expression, and we confirmed that this was the case (Fig. S8). Since metabolic changes might occur in mice that have undergone the sucrose test and these might influence LGI1 levels, we tested whether LGI1 was affected by 2% sucrose intake. The protein level of LGI1 in mice freely exposed to 2% sucrose water during the 2-day test protocol was comparable to that in mice consuming tap water (Fig. S9). Our data provide substantial evidence that neuritin interacts with IR, and that the ensuing LGI1 expression plays a key role in its antidepressant-like effects (see Fig. 7).

4. Discussion

In the light of the previous reports showing that neuronal atrophy accompanies depression (Gradin and Pomi, 2008) and that neuritin increases spine density and neurite length (Son et al., 2012), we sought to identify effector molecules that control and trigger synapse formation. LGI1 was studied as a downstream target signal since it shares the following properties with neuritin: (1) predominant localization at the synapses of the hippocampal DG (Kegel et al., 2013; Naeve et al., 1997); (2) functional significance in relation to neural excitability through expression of the potassium outward current (I_A) subunit and (3) a causal relation to neurite outgrowth (Owuor et al., 2009); (Son et al., 2012). We have shown, for the first time, that LGI1 expression is dependent on neuritin-mediated phosphorylation of HDAC5, and that the resulting LGI1 expression rescues the depression-like behaviors in the FST, NSFT and LHT. These results suggest that LGI1 may play a role in relaying the resilience to stress.

To further support a role for neuritin as an endogenous antidepressant, we manipulated neuritin levels *in vivo* by two approaches: creating *Nrn1* conditional-transgenic mice by crossing *Nrn1*$^{flox/flox}$ mice with *Pomc-cre* transgenic mice (Fig. S5), and overexpressing lentivirus-transduced *Nrn1* (Fig. 4). Mice infused with lenti-*Nrn1*-mCherry into DG had reduced depression-like behaviors after CUS in four behavioral tests sensitive to antidepressants. These results resembled the effects observed in the *Nrn1* cOE mice, revealing protection from the adverse behavioral effects of CUS in the NSFT, FST and LHT. According to this view, sucrose consumption should be enhanced in *Nrn1* cOE mice, but we failed to detect any difference in sucrose consumption between

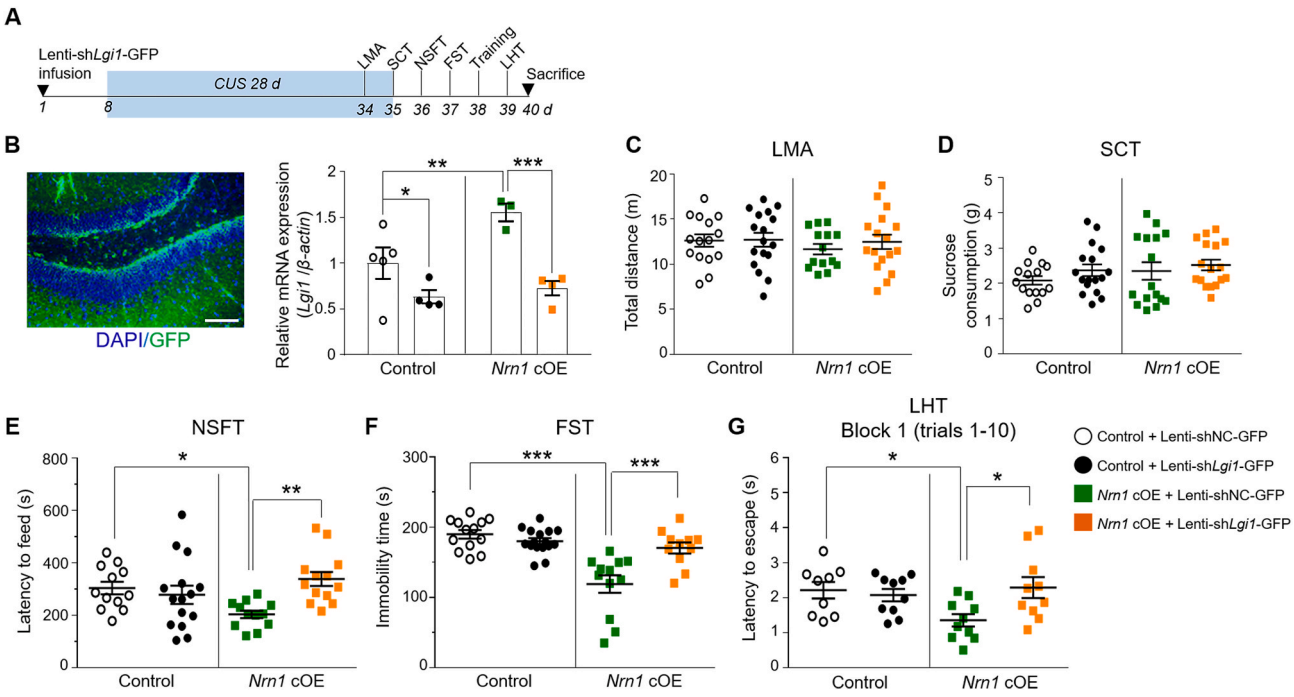

Fig. 5. Stress resilience in *Nrn1* cOE mice are abolished by LGI1 depletion. (A) Timeline of experimental procedures. Mice were injected with lenti-shNC-GFP and lenti-sh*Lgi1*-GFP and exposed to CUS for 28 d. (B) Localization of lentivirus in the hippocampal DG by GFP staining (Scale bar, 100 μm) (*Left*). *Lgi1* mRNA measured by real-time PCR (*Right*) ($n = 3$–5 per group). (C) LMA. Total distance ($n = 15$–17 per group). (D) SCT. Total sucrose consumption ($n = 15$–17 per group). (E) NSFT. Latency to feed was increased in lenti-sh*Lgi1*-GFP-infused *Nrn1* cOE mice compared with lenti-shNC-GFP-infused *Nrn1* cOE mice (n = 12–15 per group). (F) FST. Lenti-shNC-GFP-infused *Nrn1* cOE mice displayed a decrease in immobility compared with lenti-shNC-GFP-infused control mice, which was blocked by lenti-sh*Lgi1*-GFP infusion (n = 11–16 per group). (G) LHT. Lenti-shNC-GFP-infused *Nrn1* cOE mice displayed a decrease in latency to escape compared with lenti-shNC-GFP-infused control mice, which was blocked by lenti-sh*Lgi1*-GFP infusion ($n = 9$–10 per group). In (B)–(G), Data are represented as mean ± SEM; $^{*}p < 0.05$, $^{**}p < 0.01$, $^{***}p < 0.001$. Statistics: Two-way ANOVA followed by Bonferroni posttest (B and F) or Newman-Keuls posttest (E and G). Statistics detailed in Table S4.

littermate controls (*Nrn1*$^{flox/flox}$) and *Nrn1* cOE (*Nrn1*$^{flox/flox}$:*Pomc-cre*) mice exposed to CUS. In line with this, exposure of *Nrn1* cOE mice infused with lenti-sh*Lgi1*-GFP to CUS did not decrease sucrose consumption. This suggests a somewhat different underlying genetic substrate of the SCT, consistent with some of the strain-dependent sucrose/glucose/saccharin preferences and the high inter-individual variability of mice discussed previously (Pothion et al., 2004). The regimen of the sucrose consumption test might need to be modified for *Nrn1* cOE mice to see if such progressive anhedonic behaviors are elicited (Duric et al., 2010).

There is ample evidence that behavioral changes in depression and mood disorders in mice involve the phosphorylation states of HDAC5 (Choi et al., 2015; Erburu et al., 2015; Tsankova et al., 2006) and probably depend on long-lasting changes in the expression of various target genes. We demonstrated that soluble recombinant neuritin stimulated HDAC5 phosphorylation and promoted nuclear export, leading to transcriptional activity of MEF2, thereby increasing the expression of LGI1 (Fig. 2 and S4). These data were corroborated in *Nrn1* cOE mice (Fig. 3B and C). The functional state of HDAC5 signaling was assessed by analysis of p-HDAC5 in the hippocampus. Exposure to CUS decreased levels of both p-HDAC5 and LGI1 (Figs. 3B, C and 4I–4K). However, the effect of CUS was more robust and statistically significant for p-HDAC5 levels in non-stressed controls than in the *Nrn1* cOE mice (Fig. 3B). Likewise, there was no significant effects of CUS on LGI1 levels in *Nrn1* cOE mice compared to non-stressed controls (Fig. 3C). The CUS-induced decrease in LGI1 level was restored following fluoxetine treatment (Fig. 1B). Importantly, the reduced levels of p-HDAC5 and LGI1 in CUS were completely rescued in mice in which neuritin was virally overexpressed and in *Nrn1* cOE mice (Figs. 3B, C and 4I–4K). Since the effects of neuritin on phosphorylating HDAC5 and gene expression became apparent on exposure to CUS rather than in the home cage, it is consistent with our previous finding that neuritin rescues the behavioral and morphological deficits caused by CUS (Son et al., 2012). When we sought to understand the effects of p-HDAC5 levels on depression-like behaviors, as observed especially in the LHT (Fig. 3I), we only observed a non-significant trend in the association between latency to escape × p-HDAC5, indicating that the level of p-HDAC5 is only partially indicative of CUS-induced behavioral phenotypes.

There is difference in the effect of neuritin on HDAC5 phosphorylation in vitro and *in vivo*: whereas neuritin increases p-HDAC5 in a dose-dependent manner in vitro, *Nrn1* cOE mice display an increase in p-HDAC5 only in CUS, not under non-stressed condition. Given that neuritin is expressed in an activity-dependent manner and localizes to hippocampal synapses (Shimada et al., 2016), its effect on HDAC5 phosphorylation might require concurrent synaptic activity, and it may have most effect when synaptic activity is decreased under CUS. Neuritin might have only dose-dependent effects on HDAC5 phosphorylation in vitro.

Using a complementary approach, we knocked down *Lgi1* specifically in the DG using lentiviruses and assessed the effects on mouse behaviors. In the absence of CUS, lenti-sh*Lgi1*-GFP significantly increased behavioral measures (: immobility) in both littermate controls and *Nrn1* cOE mice in the FST (Fig. S7E), suggesting a potential role for LGI1 as an endogenous regulator in maintaining mood-related responses. Depletion of LGI1 in the DG did not itself cause further depression but could oppose the antidepressant effects of neuritin in CUS (Fig. 5E-G), thus supporting an important role for neuritin-induced LGI1 levels in maintaining behavioral resilience to challenge under CUS, and their essential role in the presumed antidepressant actions of neuritin. Further investigation is needed to evaluate the physiological and pathological relevance of LGI1 in stress-induced behavioral defects.

It was recently shown that human autoantibodies against LGI1 (patient-derived IgG), when infused into mice, reduced the synaptic level of $K_V1.1$, and produced an impairment of long-term potentiation in the

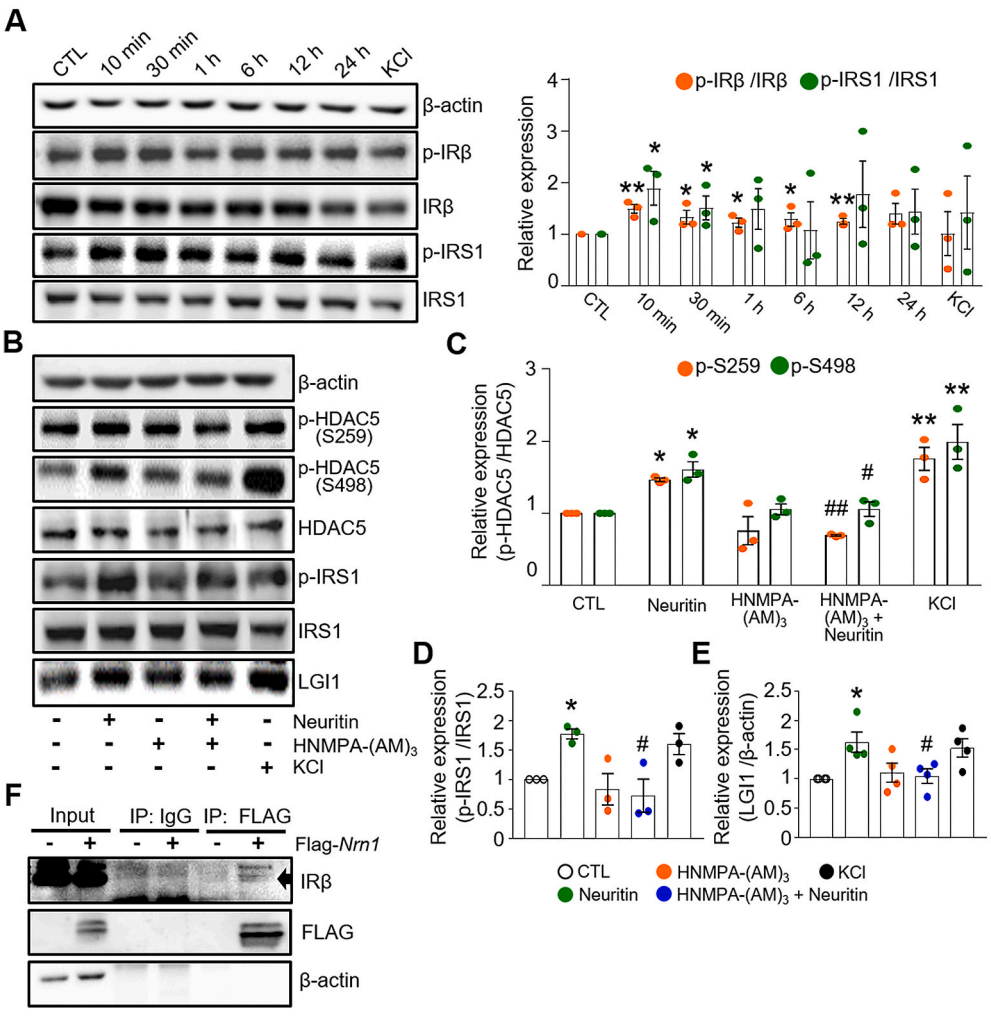

Fig. 6. Neuritin mediates LGI1 expression through insulin receptors. (A) Representative immunoblots of neurons (DIV7) treated with 200 ng/ml recombinant soluble neuritin for various times, or 30 mM KCl for 6 h. Quantitative data for p-IRβ Y1135/1136 or p-IRS1 Y608 expression ($n = 3$). (B and C) Representative immunoblots of neurons pretreated with 100 μM HNMPA-$(AM)_3$ for 30 min and stimulated with recombinant soluble neuritin for 30 min. Quantitative data of HDAC5 phosphorylation expression ($n = 3$). (B and D) Representative immunoblots of neurons pretreated with 100 μM HNMPA-$(AM)_3$ for 30 min and stimulated with recombinant soluble neuritin for 10 min. Quantitative data for p-IRS1 Y608 expression ($n = 3$). (B and E) Representative immunoblots of neurons pretreated with 100 μM HNMPA-$(AM)_3$ for 30 min and stimulated with recombinant soluble neuritin for 6 h. Quantitative data for LGI1 expression ($n = 4$). (F) Co-immunoprecipitation of neuritin-IR complexes. HEK293T cells expressing the Flag-*Nrn1* construct were subjected to IP using anti-FLAG antibody. Both inputs and co-IP fractions (IP α-FLAG) were immunoblotted with anti-IRβ or anti-FLAG antibodies (black arrow: IRβ). IRβ was co-immunoprecipitated with anti-FLAG antibody. In (A)–(E), Data are represented as mean ± SEM; $^{*}p < 0.05$, $^{**}p < 0.01$, $^{***}p < 0.001$ compared with CTL, $^{\#}p < 0.05$, $^{\#\#}p < 0.01$, $^{\#\#\#}p < 0.001$ compared with recombinant soluble neuritin treatment. Statistics: Student's *t*-test (A). One-way ANOVA followed by Newman-Keuls posttest test (C, D and E). Statistics detailed in Table S4.

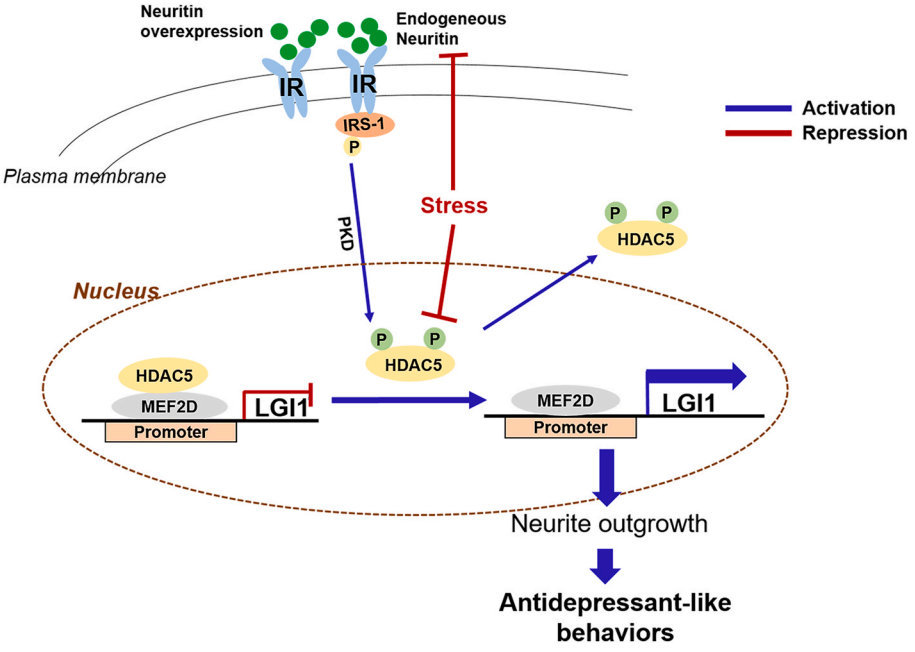

Fig. 7. A schematic of proposed mechanisms for the antidepressant-like effects of neuritin acting via LGI1. Chronic stress reduces neuritin expression and HDAC5 phosphorylation. Normally MEF2 associates with HDAC5 and blocks its nuclear export, which results in repression of MEF2 transcriptional activity. Neuritin stimulates phosphorylation of IR and IRS-1, leading to PKD activation. HDAC5 is phosphorylated in a PKD-dependent pathway, which is followed by nuclear export of p-HDAC5. This leads to reduced binding of HDAC5 to the *Lgi1* promoter, thereby derepressing LGI1 expression. LGI1 increases neurite outgrowth and may restore other neuronal signaling. As a result, the depressive behaviors induced by chronic stress are rescued.

CA1 region of the hippocampus and a memory deficit (Petit-Pedrol et al., 2018). LGI1, as an extracellular factor, increases neurite outgrowth (Fukata et al., 2006; Owuor et al., 2009) and determines the precise location of PSD-95 in the synapse, and, in turn, reinforces receptor clustering in the synapse (Fukata et al., 2021). According to Sholl analysis in the present study, *Lgi1* knockdown reduces neurite complexity over the entire proximal to distal area of the soma. Soluble neuritin rescued neurite outgrowth at ≥50 μm away from the soma, where the perforant path forms synapses with GCs (Fig. 1F). We speculate that CUS (or *Lgi1* knockdown in GCs) results in reduced release of LGI1 into synaptic clefts. As a result, transsynaptic protein networks, including Kv1.1 and glutamate receptors, are altered at the synapse, resulting in the decreased frequency of mEPSCs recorded in GCs (Fig. S6). Since LGI1 is predominantly expressed in the outer and middle molecular layers of the GC, the CUS-induced decrease in LGI1 may exacerbate the deleterious effects of stress on GCs.

Deficiencies in IR activation and downstream IR-related mechanisms may result in aberrant IR-mediated functions and lead to a broad range of brain disorders, including neuropsychiatric disorders such as depression (Pomytkin et al., 2018). In view of this, it is of particular importance that neuritin-induced IR activation, the resulting HDAC5 phosphorylation and LGI1 expression contributed to the antidepressant-like effects of neuritin. This is substantiated by the observation that neuritin-induced LGI1 activation is blocked by HNMPA-$(AM)_3$, an antagonist of the IR (Fig. 6B and E), and that both neuritin and insulin similarly activate insulin receptor signaling pathways (Fig. 6A, S8A and S8B). Indeed, insulin also increases PKD and HDAC5 phosphorylation and LGI1 expression (Figs. S8C–S8E). Although neuritin and insulin both elicit the immediate effects of IR activation, neuritin might interact with IR in a way that differs from insulin. The co-IP of neuritin with IR could depend on the formation of a multi-protein complex rather than a direct, interaction with IR (Fig. 6F). Conceivably, neuritin, by affecting the tyrosine kinase receptor, contributes to the brain pathology underlying depression associated with diabetes. This idea is supported by the prevalence of depression in diabetic patients (Gendelman et al., 2009) and, conversely, the high incidence of diabetes in depressed patients (Reus et al., 2017), who lack fibroblast growth factor (FGF). With regard to metabolic processes, neuritin may cooperate with insulin to control or alleviate depression by regulating activation of tyrosine kinase receptors and ultimately controlling gene expression via HDAC5. In line with this, it is noticeable that insulin receptor sensitizers are reported to be effective in treating MDD that is refractory to standard antidepressant treatment and accompanied by insulin resistance (Pomytkin et al., 2018). Based on this and our observations, further studies are warranted of the following points: (1) whether IR-A, which is exclusively expressed in neurons, and IR-B, the predominant form in peripheral tissues, are differentially involved during CUS and in stress-related neuropsychiatric disorders including MDD; (2) the effect of primary IR autophosphorylation on LGI1 expression during CUS; (3) and, of great interest, whether insulin receptor sensitizers induce LGI1 in the hippocampus. In addition, identification of the neuritin interactome should greatly benefit our understanding of how neuronal activity is modified, and help develop further effective interventions for MDD.

Our study has several limitations. First, in order to determine whether the transgene produces an "antidepressant-like" reversal of a pre-existing deficit, the lenti-transgene ought to be administered *after* CUS followed by observation of the behavioral deficits induced by CUS. However, this was difficult to achieve given the need for lentivirus infusion to be performed under anesthetic surgery, since the latter requires a recovery period of several days, whereas the behavioral consequences should be observed without delay, at the time of maximal expression of the lenti-transgene. Therefore, we infused lentivirus into the hippocampus 1–2 wks prior to CUS rather than after CUS. This protocol, involving expressing the transgene before the start of CUS and coincident with the period of CUS, essentially enables us to observe the effect of the transgene on resilience to CUS. Second, we investigated the consequences of overexpressing neuritin in the hippocampus by two approaches: examining *Nrn1*-conditional Tg mice by crossing floxed *Nrn1* mice with *Pomc-cre* transgenic mice and overexpressing virus-transduced *Nrn1*. Because *Pomc*-cre-mediated recombination during embryonic development results in *Nrn1* overexpression throughout adulthood, *Nrn1* may be overexpressed in off-target sites that could confound the analysis of the contribution of neuritin overexpression to the resulting phenotypes. Viral-mediated *Nrn1* overexpression allowed us to specifically assess *Nrn1* function in the postnatal forebrain without interfering with its contribution to early CNS development. Third, we focused on LGI1's activity in the hippocampal DG region where it is predominantly expressed in the outer and middle molecular layers (OML and MML) (Schulte et al., 2006). The localization of LGI1 is of particular importance because of previous findings that the MML, which is located 50 μm from the granule cell body in the DG, shows dynamic behavior following stress and antidepressant treatment (Kitahara et al., 2016). Lastly, the present study was confined to male mice since it appears that only males suffer behavioral impairments accompanied by morphological deficits in neurons after 28 days of CUS (Woodburn et al., 2021). Based on the higher incidence of depression in women, further investigations of gender differences in the regulatory functions of neuritin, including IR activation in the MDD, are warranted.

Overall, neuritin-mediated LGI1 expression plays a critical role in ameliorating pathological depression. The mechanisms of action by which LGI1, as a downstream target of neuritin signaling, mediates mood-related behaviors and hippocampal synaptic efficacy warrant further investigation.

Correspondence and request for material

Any request for data or code should be addressed to J.-H.K. and H.S.

CRediT authorship contribution statement

Seung Hoon Lee: Conceptualization, Methodology, Validation, Formal analysis, Investigation, Data curation, Visualization, Writing – original draft, Writing – review & editing. **Nam-Shik Kim:** Conceptualization, Methodology, Investigation, Resources. **Miyeon Choi:** Investigation, Visualization, Funding acquisition. **Seung Yeon Ko:** Investigation, Funding acquisition. **Sung Eun Wang:** Investigation. **Hye-Ryeong Jo:** Investigation. **Jee Young Seo:** Investigation. **Yong-Seok Kim:** Resources. **Hyun Jin Kim:** Investigation. **Hyun-Yong Lee:** Investigation. **Joung-Hun Kim:** Conceptualization, Methodology, Supervision, Writing – review & editing, Funding acquisition. **Hyeon Son:** Conceptualization, Methodology, Supervision, Writing – original draft, Writing – review & editing, Project administration, Funding acquisition.

Declaration of competing interest

The authors declare that they have no known competing financial interests or personal relationships that could have appeared to influence the work reported in this paper.

Acknowledgments

This work was supported by National Research Foundation of Korea Grants (No. 2016R1A2B2006474 and No. 2019R1A2C2003616 to H.S.); Basic Science Research Program Grants (No. 2017R1D1A1B03032858 to M.C., No. 2019R1A6A3A01092534 to S.Y.K.); Brain Research Program (No. 2018M3C7A1024152 to J.-H.K.); Research Leader Program (No. 2018R1A3B1052079 to J.-H.K.) and a Medical Research Center Grant (No. 2017R1A5A2015395 to H.S.) funded by the Ministry of Science and Technology, Republic of Korea.

Appendix A. Supplementary data

Supplementary data to this article can be found online at https://doi.org/10.1016/j.ynstr.2021.100373.

References

An, K., Jung, J.H., Jeong, A.Y., Kim, H.G., Jung, S.Y., Lee, K., Kim, H.J., Kim, S.J., Jeong, T.Y., Son, Y., Kim, H.S., Kim, J.H., 2014. Neuritin can normalize neural deficits of Alzheimer's disease. Cell Death Dis. 5, e1523. https://doi.org/10.1038/cddis.2014.478.

Andres, V., Cervera, M., Mahdavi, V., 1995. Determination of the consensus binding site for MEF2 expressed in muscle and brain reveals tissue-specific sequence constraints. J. Biol. Chem. 270, 23246–23249.

Barbosa, A.C., Kim, M.S., Ertunc, M., Adachi, M., Nelson, E.D., McAnally, J., Richardson, J.A., Kavalali, E.T., Monteggia, L.M., Bassel-Duby, R., Olson, E.N., 2008. MEF2C, a transcription factor that facilitates learning and memory by negative regulation of synapse numbers and function. Proc. Natl. Acad. Sci. U. S. A. 105, 9391–9396. https://doi.org/10.1073/pnas.0802679105.

Boillot, M., Lee, C.Y., Allene, C., Leguern, E., Baulac, S., Rouach, N., 2016. LGI1 acts presynaptically to regulate excitatory synaptic transmission during early postnatal development. Sci. Rep. 6, 21769. https://doi.org/10.1038/srep21769.

Carrasquillo, Y., Burkhalter, A., Nerbonne, J.M., 2012. A-type K+ channels encoded by Kv4.2, Kv4.3 and Kv1.4 differentially regulate intrinsic excitability of cortical pyramidal neurons. J. Physiol. 590, 3877–3890. https://doi.org/10.1113/jphysiol.2012.229013.

Chang, C.W., Lee, L., Yu, D., Dao, K., Bossuyt, J., Bers, D.M., 2013. Acute beta-adrenergic activation triggers nuclear import of histone deacetylase 5 and delays G(q)-induced transcriptional activation. J. Biol. Chem. 288, 192–204. https://doi.org/10.1074/jbc.M112.382358.

Choi, M., Lee, S.H., Park, M.H., Kim, Y.S., Son, H., 2017. Ketamine induces brain-derived neurotrophic factor expression via phosphorylation of histone deacetylase 5 in rats. Biochem. Biophys. Res. Commun. 489, 420–425. https://doi.org/10.1016/j.bbrc.2017.05.157.

Choi, M., Lee, S.H., Wang, S.E., Ko, S.Y., Song, M., Choi, J.S., Kim, Y.S., Duman, R.S., Son, H., 2015. Ketamine produces antidepressant-like effects through phosphorylation-dependent nuclear export of histone deacetylase 5 (HDAC5) in rats. Proc. Natl. Acad. Sci. U. S. A. 112, 15755–15760. https://doi.org/10.1073/pnas.1513913112.

Choi, Y., Lee, K., Ryu, J., Kim, H.G., Jeong, A.Y., Woo, R.S., Lee, J.H., Hyun, J.W., Hahn, S., Kim, J.H., Kim, H.S., 2014. Neuritin attenuates cognitive function impairments in tg2576 mouse model of Alzheimer's disease. PloS One 9, e104121. https://doi.org/10.1371/journal.pone.0104121.

Duman, C.H., Schlesinger, L., Kodama, M., Russell, D.S., Duman, R.S., 2007. A role for MAP kinase signaling in behavioral models of depression and antidepressant treatment. Biol. Psychiatr. 61, 661–670. https://doi.org/10.1016/j.biopsych.2006.05.047.

Duric, V., Banasr, M., Licznerski, P., Schmidt, H.D., Stockmeier, C.A., Simen, A.A., Newton, S.S., Duman, R.S., 2010. A negative regulator of MAP kinase causes depressive behavior. Nat. Med. 16, 1328–1332. https://doi.org/10.1038/nm.2219.

Erburu, M., Munoz-Cobo, I., Dominguez-Andres, J., Beltran, E., Suzuki, T., Mai, A., Valente, S., Puerta, E., Tordera, R.M., 2015. Chronic stress and antidepressant induced changes in Hdac5 and Sirt2 affect synaptic plasticity. Eur. Neuropsychopharmacol 25, 2036–2048. https://doi.org/10.1016/j.euroneuro.2015.08.016.

Flavell, S.W., Cowan, C.W., Kim, T.K., Greer, P.L., Lin, Y., Paradis, S., Griffith, E.C., Hu, L. S., Chen, C., Greenberg, M.E., 2006. Activity-dependent regulation of MEF2 transcription factors suppresses excitatory synapse number. Science 311, 1008–1012. https://doi.org/10.1126/science.1122511.

Flavell, S.W., Kim, T.K., Gray, J.M., Harmin, D.A., Hemberg, M., Hong, E.J., Markenscoff-Papadimitriou, E., Bear, D.M., Greenberg, M.E., 2008. Genome-wide analysis of MEF2 transcriptional program reveals synaptic target genes and neuronal activity-dependent polyadenylation site selection. Neuron 60, 1022–1038. https://doi.org/10.1016/j.neuron.2008.11.029.

Fujino, T., Wu, Z., Lin, W.C., Phillips, M.A., Nedivi, E., 2008. cpg15 and cpg15-2 constitute a family of activity-regulated ligands expressed differentially in the nervous system to promote neurite growth and neuronal survival. J. Comp. Neurol. 507, 1831–1845. https://doi.org/10.1002/cne.21649.

Fukata, Y., Adesnik, H., Iwanaga, T., Bredt, D.S., Nicoll, R.A., Fukata, M., 2006. Epilepsy-related ligand/receptor complex LGI1 and ADAM22 regulate synaptic transmission. Science 313, 1792–1795. https://doi.org/10.1126/science.1129947.

Fukata, Y., Chen, X., Chiken, S., Hirano, Y., Yamagata, A., Inahashi, H., Sanbo, M., Sano, H., Goto, T., Hirabayashi, M., Kornau, H.C., Pruss, H., Nambu, A., Fukai, S., Nicoll, R.A., Fukata, M., 2021. LGI1-ADAM22-MAGUK configures transsynaptic nanoalignment for synaptic transmission and epilepsy prevention. Proc. Natl. Acad. Sci. U. S. A. 118 https://doi.org/10.1073/pnas.2022580118.

Fukata, Y., Lovero, K.L., Iwanaga, T., Watanabe, A., Yokoi, N., Tabuchi, K., Shigemoto, R., Nicoll, R.A., Fukata, M., 2010. Disruption of LGI1-linked synaptic complex causes abnormal synaptic transmission and epilepsy. Proc. Natl. Acad. Sci. U. S. A. 107, 3799–3804. https://doi.org/10.1073/pnas.0914537107.

Gendelman, N., Snell-Bergeon, J.K., McFann, K., Kinney, G., Paul Wadwa, R., Bishop, F., Rewers, M., Maahs, D.M., 2009. Prevalence and correlates of depression in individuals with and without type 1 diabetes. Diabetes Care 32, 575–579. https://doi.org/10.2337/dc08-1835.

Gradin, V.B., Pomi, A., 2008. The role of hippocampal atrophy in depression: a neurocomputational approach. J. Biol. Phys. 34, 107–120. https://doi.org/10.1007/s10867-008-9099-7.

Guise, A.J., Mathias, R.A., Rowland, E.A., Yu, F., Cristea, I.M., 2014. Probing phosphorylation-dependent protein interactions within functional domains of histone deacetylase 5 (HDAC5). Proteomics 14, 2156–2166. https://doi.org/10.1002/pmic.201400092.

Karamoysoyli, E., Burnand, R.C., Tomlinson, D.R., Gardiner, N.J., 2008. Neuritin mediates nerve growth factor-induced axonal regeneration and is deficient in experimental diabetic neuropathy. Diabetes 57, 181–189. https://doi.org/10.2337/db07-0895.

Kegel, L., Aunin, E., Meijer, D., Bermingham, J.R., 2013. LGI proteins in the nervous system. ASN Neuro 5, 167–181. https://doi.org/10.1042/AN20120095.

Kitahara, Y., Ohta, K., Hasuo, H., Shuto, T., Kuroiwa, M., Sotogaku, N., Togo, A., Nakamura, K., Nishi, A., 2016. Chronic fluoxetine induces the enlargement of perforant path-granule cell synapses in the mouse dentate gyrus. PloS One 11, e0147307. https://doi.org/10.1371/journal.pone.0147307.

Ko, S.Y., Wang, S.E., Lee, H.K., Jo, S., Han, J., Lee, S.H., Choi, M., Jo, H.R., Seo, J.Y., Jung, S.J., Son, H., 2019. Transient receptor potential melastatin 2 governs stress-induced depressive-like behaviors. Proc. Natl. Acad. Sci. U. S. A. 116, 1770–1775. https://doi.org/10.1073/pnas.1814335116.

Koo, J.W., Russo, S.J., Ferguson, D., Nestler, E.J., Duman, R.S., 2010. Nuclear factor-kappaB is a critical mediator of stress-impaired neurogenesis and depressive behavior. Proc. Natl. Acad. Sci. U. S. A. 107, 2669–2674. https://doi.org/10.1073/pnas.0910658107.

Koran, L.M., Cain, J.W., Dominguez, R.A., Rush, A.J., Thiemann, S., 1996. Are fluoxetine plasma levels related to outcome in obsessive-compulsive disorder? Am. J. Psychiatr. 153, 1450–1454. https://doi.org/10.1176/ajp.153.11.1450.

Lee, K.-H., Ryu, C.J., Hong, H.J., Kim, J., Lee, E.H., 2005. cDNA microarray analysis of nerve growth factor-regulated gene expression profile in rat PC12 cells. Neurochem. Res. 30, 533–540. https://doi.org/10.1007/s11064-005-2688-y.

Lin, X., Shah, S., Bulleit, R.F., 1996. The expression of MEF2 genes is implicated in CNS neuronal differentiation. Brain Res. Mol. Brain Res. 42, 307–316. https://doi.org/10.1016/s0169-328x(96)00135-0.

Lovero, K.L., Fukata, Y., Granger, A.J., Fukata, M., Nicoll, R.A., 2015. The LGI1-ADAM22 protein complex directs synapse maturation through regulation of PSD-95 function. Proc. Natl. Acad. Sci. U. S. A. 112, E4129–E4137. https://doi.org/10.1073/pnas.1511910112.

Lyons, G.E., Micales, B.K., Schwarz, J., Martin, J.F., Olson, E.N., 1995. Expression of mef2 genes in the mouse central nervous system suggests a role in neuronal maturation. J. Neurosci. 15, 5727–5738.

Malykhin, N.V., Coupland, N.J., 2015. Hippocampal neuroplasticity in major depressive disorder. Neuroscience 309, 200–213. https://doi.org/10.1016/j.neuroscience.2015.04.047.

Martin, S., Henley, J.M., Holman, D., Zhou, M., Wiegert, O., van Spronsen, M., Joels, M., Hoogenraad, C.C., Krugers, H.J., 2009. Corticosterone alters AMPAR mobility and facilitates bidirectional synaptic plasticity. PloS One 4, e4714. https://doi.org/10.1371/journal.pone.0004714.

McEwen, B.S., Bowles, N.P., Gray, J.D., Hill, M.N., Hunter, R.G., Karatsoreos, I.N., Nasca, C., 2015. Mechanisms of stress in the brain. Nat. Neurosci. 18, 1353–1363. https://doi.org/10.1038/nn.4086.

McKinsey, T.A., Zhang, C.L., Lu, J., Olson, E.N., 2000a. Signal-dependent nuclear export of a histone deacetylase regulates muscle differentiation. Nature 408, 106–111. https://doi.org/10.1038/35040593.

McKinsey, T.A., Zhang, C.L., Olson, E.N., 2000b. Activation of the myocyte enhancer factor-2 transcription factor by calcium/calmodulin-dependent protein kinase-stimulated binding of 14-3-3 to histone deacetylase 5. Proc. Natl. Acad. Sci. U. S. A. 97, 14400–14405. https://doi.org/10.1073/pnas.260501497.

Naeve, G.S., Ramakrishnan, M., Kramer, R., Hevroni, D., Citri, Y., Theill, L.E., 1997. Neuritin: a gene induced by neural activity and neurotrophins that promotes neuritogenesis. Proc. Natl. Acad. Sci. U. S. A. 94, 2648–2653.

Nestler, E.J., Hyman, S.E., 2010. Animal models of neuropsychiatric disorders. Nat. Neurosci. 13, 1161–1169. https://doi.org/10.1038/nn.2647.

Owuor, K., Harel, N.Y., Englot, D.J., Hisama, F., Blumenfeld, H., Strittmatter, S.M., 2009. LGI1-associated epilepsy through altered ADAM23-dependent neuronal morphology. Mol. Cell. Neurosci. 42, 448–457. https://doi.org/10.1016/j.mcn.2009.09.008.

Perrone, J.A., Chabla, J.M., Hallas, B.H., Horowitz, J.M., Torres, G., 2004. Weight loss dynamics during combined fluoxetine and olanzapine treatment. BMC Pharmacol. 4, 27. https://doi.org/10.1186/1471-2210-4-27.

Petit-Pedrol, M., Sell, J., Planaguma, J., Mannara, F., Radosevic, M., Haselmann, H., Ceanga, M., Sabater, L., Spatola, M., Soto, D., Gasull, X., Dalmau, J., Geis, C., 2018. LGI1 antibodies alter Kv1.1 and AMPA receptors changing synaptic excitability, plasticity and memory. Brain 141, 3144–3159. https://doi.org/10.1093/brain/awy253.

Pomytkin, I., Costa-Nunes, J.P., Kasatkin, V., Veniaminova, E., Demchenko, A., Lyundup, A., Lesch, K.P., Ponomarev, E.D., Strekalova, T., 2018. Insulin receptor in the brain: mechanisms of activation and the role in the CNS pathology and treatment. CNS Neurosci. Ther. 24, 763–774. https://doi.org/10.1111/cns.12866.

Pothion, S., Bizot, J.C., Trovero, F., Belzung, C., 2004. Strain differences in sucrose preference and in the consequences of unpredictable chronic mild stress. Behav. Brain Res. 155, 135–146. https://doi.org/10.1016/j.bbr.2004.04.008.

Potthoff, M.J., Olson, E.N., 2007. MEF2: a central regulator of diverse developmental programs. Development 134, 4131–4140. https://doi.org/10.1242/dev.008367.

Reus, G.Z., Dos Santos, M.A.B., Strassi, A.P., Abelaira, H.M., Ceretta, L.B., Quevedo, J., 2017. Pathophysiological mechanisms involved in the relationship between diabetes

and major depressive disorder. Life Sci. 183, 78–82. https://doi.org/10.1016/j.lfs.2017.06.025.

Rudyk, C., Dwyer, Z., McNeill, J., Salmaso, N., Farmer, K., Prowse, N., Hayley, S., 2019. Chronic unpredictable stress influenced the behavioral but not the neurodegenerative impact of paraquat. Neurobiol. Stress 11, 100179. https://doi.org/10.1016/j.ynstr.2019.100179.

Schulte, U., Thumfart, J.O., Klocker, N., Sailer, C.A., Bildl, W., Biniossek, M., Dehn, D., Deller, T., Eble, S., Abbass, K., Wangler, T., Knaus, H.G., Fakler, B., 2006. The epilepsy-linked Lgi1 protein assembles into presynaptic Kv1 channels and inhibits inactivation by Kvbeta1. Neuron 49, 697–706. https://doi.org/10.1016/j.neuron.2006.01.033.

Shimada, T., Yoshida, T., Yamagata, K., 2016. Neuritin mediates activity-dependent axonal branch formation in part via FGF signaling. J. Neurosci. 36, 4534–4548. https://doi.org/10.1523/JNEUROSCI.1715-15.2016.

Son, H., Banasr, M., Choi, M., Chae, S.Y., Licznerski, P., Lee, B., Voleti, B., Li, N., Lepack, A., Fournier, N.M., Lee, K.R., Lee, I.Y., Kim, J., Kim, J.H., Kim, Y.H., Jung, S. J., Duman, R.S., 2012. Neuritin produces antidepressant actions and blocks the neuronal and behavioral deficits caused by chronic stress. Proc. Natl. Acad. Sci. U. S. A. 109, 11378–11383. https://doi.org/10.1073/pnas.1201191109.

Srinivas, S., Watanabe, T., Lin, C.S., William, C.M., Tanabe, Y., Jessell, T.M., Costantini, F., 2001. Cre reporter strains produced by targeted insertion of EYFP and ECFP into the ROSA26 locus. BMC Dev. Biol. 1, 4. https://doi.org/10.1186/1471-213x-1-4.

Stepanichev, M., Dygalo, N.N., Grigoryan, G., Shishkina, G.T., Gulyaeva, N., 2014. Rodent models of depression: neurotrophic and neuroinflammatory biomarkers. BioMed Res. Int. 2014, 932757. https://doi.org/10.1155/2014/932757.

Thomas, R.A., Gibon, J., Chen, C.X.Q., Chierzi, S., Soubannier, V.G., Baulac, S., Seguela, P., Murai, K., Barker, P.A., 2018. The Nogo receptor ligand LGI1 regulates synapse number and synaptic activity in hippocampal and cortical neurons. eNeuro 5. https://doi.org/10.1523/ENEURO.0185-18.2018.

Tsankova, N.M., Berton, O., Renthal, W., Kumar, A., Neve, R.L., Nestler, E.J., 2006. Sustained hippocampal chromatin regulation in a mouse model of depression and antidepressant action. Nat. Neurosci. 9, 519–525. https://doi.org/10.1038/nn1659.

Vega, R.B., Harrison, B.C., Meadows, E., Roberts, C.R., Papst, P.J., Olson, E.N., McKinsey, T.A., 2004. Protein kinases C and D mediate agonist-dependent cardiac hypertrophy through nuclear export of histone deacetylase 5. Mol. Cell Biol. 24, 8374–8385. https://doi.org/10.1128/MCB.24.19.8374-8385.2004.

Woodburn, S.C., Bollinger, J.L., Wohleb, E.S., 2021. Synaptic and behavioral effects of chronic stress are linked to dynamic and sex-specific changes in microglia function and astrocyte dystrophy. Neurobiol. Stress 14, 100312. https://doi.org/10.1016/j.ynstr.2021.100312.

Yao, J.J., Zhao, Q.R., Liu, D.D., Chow, C.W., Mei, Y.A., 2016. Neuritin up-regulates Kv4.2 alpha-subunit of potassium channel expression and affects neuronal excitability by regulating the calcium-calcineurin-NFATc4 signaling pathway. J. Biol. Chem. 291, 17369–17381. https://doi.org/10.1074/jbc.M115.708883.

Yuen, E.Y., Liu, W., Karatsoreos, I.N., Feng, J., McEwen, B.S., Yan, Z., 2009. Acute stress enhances glutamatergic transmission in prefrontal cortex and facilitates working memory. Proc. Natl. Acad. Sci. U. S. A. 106, 14075–14079. https://doi.org/10.1073/pnas.0906791106.

Zito, A., Cartelli, D., Cappelletti, G., Cariboni, A., Andrews, W., Parnavelas, J., Poletti, A., Galbiati, M., 2014. Neuritin 1 promotes neuronal migration. Brain Struct. Funct. 219, 105–118. https://doi.org/10.1007/s00429-012-0487-1.